HHS Public Access

Author manuscript

Sci Transl Med. Author manuscript; available in PMC 2024 January 01.

Published in final edited form as:

Sci Transl Med. 2023 June 21; 15(701): eadd7872. doi:10.1126/scitranslmed.add7872.

BLM overexpression as a predictive biomarker for CHK1 inhibitor response in PARP inhibitor–resistant *BRCA*-mutant ovarian cancer

Nitasha Gupta[1,†], **Tzu-Ting Huang**[1,†], **Jayakumar R. Nair**[1,†], **Daniel An**[1], **Grant Zurcher**[1], **Erika J. Lampert**[1,2], **Ann McCoy**[1], **Ashley Cimino-Mathews**[3], **Elizabeth M. Swisher**[4], **Marc R. Radke**[4], **Christina M. Lockwood**[4,5], **Jonathan B. Reichel**[4], **Chih-Yuan Chiang**[6], **Kelli M. Wilson**[6], **Ken Chih-Chien Cheng**[6], **Darryl Nousome**[7], **Jung-Min Lee**[1,*]

[1]Women's Malignancies Branch, Center for Cancer Research (CCR), National Cancer Institute (NCI), National Institutes of Health (NIH), Bethesda, MD 20892, USA.

[2]Department of Obstetrics and Gynecology, Cleveland Clinic, Cleveland, OH 44195, USA.

[3]Departments of Pathology and Oncology, Johns Hopkins University School of Medicine, Baltimore, MD 21231, USA.

[4]Brotman Baty Institute of Precision Medicine, University of Washington, Seattle, WA 98195, USA.

[5]Department of Laboratory Medicine and Pathology, University of Washington, Seattle, WA 98195, USA.

[6]National Center for Advancing Translational Sciences, National Institutes of Health (NIH), Rockville, MD 20892, USA.

[7]Center for Cancer Research Collaborative Bioinformatics Resource, Center for Cancer Research (CCR), National Cancer Institute (NCI), National Institutes of Health (NIH), Bethesda, MD 20892, USA.

Abstract

Poly(ADP-ribose) polymerase inhibitors (PARPis) have changed the treatment paradigm in breast cancer gene (*BRCA*)–mutant high-grade serous ovarian carcinoma (HGSC). However, most patients eventually develop resistance to PARPis, highlighting an unmet need for improved

*Corresponding author. leej6@mail.nih.gov.
†These authors contributed equally to this work.

Author contributions: Conceptualization: N.G., T.-T.H., J.R.N., and J.-M.L. Methodology: N.G., T.-T.H., J.R.N., J.B.R., C.-Y.C., K.M.W., and D.N. Investigation: N.G., T.-T.H., J.R.N., and J.-M.L. Visualization: N.G., T.-T.H., J.R.N., D.N., K.M.W., and J.B.R. Funding acquisition: J.-M.L., E.M.S., N.G., T.-T.H., and K.C.-C.C. Project administration: J.-M.L. Supervision: J.-M.L. Writing—original draft: N.G., T.-T.H., J.R.N., and J.-M.L. Writing—review and editing: N.G., T.-T.H., J.R.N., D.A., G.Z., E.J.L., A.M., A.C.-M., E.M.S., M.R.R., C.M.L., J.B.R., C.-Y.C., K.M.W., K.C.-C.C., D.N., J.-M.L.

Competing interests: E.M.S. is on the Data and Safety Monitoring Board of Novartis and Scientific Advisory Board of Ideaya Bioscience. A.C.-M. has research grant funding from Bristol-Myers Squibb (paid to institution). J.-M.L. has research grant funding from AstraZeneca and Acrivon Therapeutics (paid to institution) and is on the Scientific Advisory Board of Acrivon Therapeutics (unpaid). The other authors declare that they have no competing interests.

Data and materials availability: All data associated with this study are present in the paper or the Supplementary Materials. RNA-seq data are available in Dryad public data repository (doi:10.5061/dryad.18931zd2s). The PARPi-resistant cell lines (PEO1/OlaJR and UWB/OlaR) are available via material transfer agreement by contacting J.-M.L. (leej6@mail.nih.gov).

therapeutic strategies. Using high-throughput drug screens, we identified ataxia telangiectasia and rad3-related protein/checkpoint kinase 1 (CHK1) pathway inhibitors as cytotoxic and further validated the activity of the CHK1 inhibitor (CHK1i) prexasertib in PARPi-sensitive and -resistant *BRCA*-mutant HGSC cells and xenograft mouse models. CHK1i monotherapy induced DNA damage, apoptosis, and tumor size reduction. We then conducted a phase 2 study (NCT02203513) of prexasertib in patients with *BRCA*-mutant HGSC. The treatment was well tolerated but yielded an objective response rate of 6% (1 of 17; one partial response) in patients with previous PARPi treatment. Exploratory biomarker analyses revealed that replication stress and fork stabilization were associated with clinical benefit to CHK1i. In particular, overexpression of Bloom syndrome RecQ helicase (*BLM*) and cyclin E1 (*CCNE1*) overexpression or copy number gain/amplification were seen in patients who derived durable benefit from CHK1i. *BRCA* reversion mutation in previously PARPi-treated *BRCA*-mutant patients was not associated with resistance to CHK1i. Our findings suggest that replication fork–related genes should be further evaluated as biomarkers for CHK1i sensitivity in patients with *BRCA*-mutant HGSC.

INTRODUCTION

High-grade serous ovarian carcinoma (HGSC), a lethal form of ovarian cancer, often presents at advanced stages, with 80% of patients experiencing recurrences after initial therapy (1). Nearly half of HGSCs exhibit deficiency in homologous recombination (HR) DNA repair due to defects in breast cancer gene 1 (*BRCA1*) or breast cancer gene 2 (*BRCA2*) and other HR-related genes, making them ideal candidates for poly(ADP-ribose) polymerase inhibitor (PARPi)–based therapies (2, 3). Eventually, most patients discontinue PARPis because of progression, and the optimal management of PARPi-resistant HGSC is a pressing clinical challenge. To date, clinical studies have characterized several mechanisms of resistance to PARPis that include restoration of HR repair by *BRCA* or RAD51 recombinase (*RAD51*) reversion mutations, over-expression of *BRCA* hypomorphs, and other epigenetic means (4). However, little is known about other resistance mechanisms prevalent in PARPi-resistant HGSC, highlighting the importance of identifying biomarkers that can help predict response to therapies.

Among the known resistance pathways exploited by PARPi-resistant tumors (5), replication fork stabilization, an outcome of increased fork protection from degradation such as loss of paired box interacting protein 1 or loss of schlafen family member 11 or cell cycle checkpoint activation (4), is a major cause of PARPi resistance. It has been extensively studied in cell line models, but its validity and applicability as a biomarker in the clinical setting remain elusive (5).

In addition, the ataxia telangiectasia and rad3-related protein (ATR)/checkpoint kinase 1 (CHK1) pathway has been investigated in relation to DNA replication and fork stabilization (6). For instance, ATR and CHK1 phosphorylate MUS81 structure–specific endonuclease subunit (MUS81) (7) and helicases, including SWI/SNF-related, matrix-associated, actin-dependent regulator of chromatin, subfamily A–like 1 (8), and minichromosome maintenance 2–7 complex (9), thereby suppressing their activities and limiting fork reversal for replication fork stabilization. Studies have also identified overexpression of the ATR/

CHK1 pathway in PARPi-resistant or platinum-resistant HGSC (10, 11). Furthermore, HGSC has a nearly universal *TP53* mutation (2), thus disrupting the G1/S cell cycle checkpoint and rendering it more dependent on the ATR/CHK1-mediated G2/M checkpoint for DNA repair, making ATR/CHK1 signaling an attractive treatment target in *BRCA*-mutant PARPi-resistant tumors (10, 11). However, earlier clinical trials using ATR/CHK1 pathway blockade as monotherapy have revealed only modest clinical activity (6). For example, berzosertib (M6620) monotherapy yielded a response rate of 6% in patients with advanced or recurrent solid tumors that progressed on PARPis (12), highlighting the need for predictive biomarkers.

In the current study, on the basis of our preclinical findings using PARPi-resistant HGSC cells (13), we hypothesized that patients with PARPi-resistant *BRCA*-mutant HGSC would gain clinical benefit from CHK1 inhibitor (CHK1i) treatment and that biomarkers associated with replication fork dynamics would predict this clinical benefit. We tested the clinical activity and safety of the CHK1i prexasertib in heavily pretreated patients with *BRCA*-mutant HGSC, most with acquired PARPi resistance (NCT02203513). Our correlative studies also examined potential biomarkers associated with replication fork stabilization, such as the Bloom syndrome RecQ helicase (BLM), which is essential for DNA resection and replication fork protection (14). The results of the clinical trial presented here are the first demonstration of replication fork–related biomarkers that may predict clinical benefit to CHK1i in PARPi-resistant *BRCA*-mutant HGSC.

RESULTS

High-throughput drug screening identifies cell cycle checkpoint inhibitors as active drugs in PARPi-resistant *BRCA*-mutant ovarian cancer cell lines

To identify drug candidates for PARPi-resistant HGSC, we first performed high-throughput single-agent drug screening using the National Center for Advancing Translational Sciences mechanism interrogation plate (MIPE) 5.0 library of 2450 compounds (15) in three *BRCA2*-mutant HGSC cell lines, i.e., acquired PARPi–resistant PEO1/OlaR (16) along with its parental PEO1 (*BRCA2* mutation 5193C>G [Y1655X]) and de novo PARPi–resistant PEO4 (*BRCA2* reversion mutation 5193C>T [Y1655Y]) (table S1). Among others, 1082 oncology drugs, both approved and investigational, were prioritized on the basis of their status in clinical trial development (Fig. 1A and table S1). The *Z*-transformed area under the curve (*Z*-AUC) (15) was used to distinguish inactive and active drug responses. Drugs with average *Z*-AUC values less than −1.0 in all three cell lines were classified as “hits,” resulting in 151 oncology drug hits (table S2). The screen also confirmed cross-resistance between olaparib and other PARPis (rucaparib, niraparib, and talazoparib) in PARPi-resistant PEO1/OlaR and PEO4 (Fig. 1A and table S1). Drugs against cell cycle checkpoint pathways were the most enriched in the hits (20.5%, 31 of 151), followed by those targeting DNA replication (15.2%, 23 of 151), tubulin modulation (13.2%, 20 of 151), the phosphoinositide 3-kinase/protein kinase B (AKT) pathway (11.9%, 18 of 151), and DNA repair (6.0%, 9 of 151) (Fig. 1B and table S2). Among the cell cycle check-point pathway inhibitors, prexasertib was ranked in the top 15 across all oncology drug hits and demonstrated

substantial cytotoxicity in all cell lines (rank 15; table S2); therefore, it was selected for subsequent preclinical studies and a clinical trial.

We further validated the findings from the drug screen using six *BRCA*-mutant HGSC cell lines, including four *BRCA2*-mutant [PEO1, PEO1/OlaR, and PEO4 as described above, plus another acquired PARPi–resistant PEO1/OlaJR (13)] and two *BRCA1*-mutant PARPi-sensitive [UWB1.289 (UWB)] and -resistant (UWB/OlaR) cell lines. Median inhibitory concentration (IC_{50}) values against olaparib were at least eightfold higher in PARPi-resistant *BRCA*-mutant cells, ranging from 26.3 to >50 μM relative to their parental cells (UWB and PEO1, IC_{50} 3.4 and 4.9 μM, respectively; Fig. 1C, top). IC_{50} values for prexasertib monotherapy ranged from 1.2 to 30.6 nM in PARPi-sensitive and -resistant *BRCA*-mutant HGSC cells (Fig. 1C, bottom). Using clinically attainable concentrations of prexasertib (0.125 to 100 nM) (17), CHK1i alone decreased the colony-forming ability in both PARPi-sensitive and PARPi-resistant cells (Fig. 1D), whereas the combination with olaparib did not yield synergism in all six HGSC cells (fig. S1, A and B), consistent with a previous report in models of xenografts derived from patients with *BRCA1*-mutant PARPi-resistant HGSC (18). Last, immunoblotting showed that prexasertib inhibited CHK1 activation (lower p-CHK1 S296) in all cell lines (Fig. 1E), indicating a target effect.

CHK1 inhibition induces lethal replication stress and DNA damage in PARPi-resistant *BRCA*-mutant HGSC cells

CHK1 plays an important role in replication fork stabilization and HR repair (6). We therefore hypothesized that the cytotoxicity of CHK1i monotherapy in PARPi-resistant HGSC cells would be associated with replication fork destabilization and impaired HR repair. To test this hypothesis, DNA fiber assays were performed by incubating cells with 5-chloro-2′-deoxyuridine (CldU) followed by 5-iodo-2′-deoxyuridine (IdU), followed by treatment with or without CHK1i and PARPi (olaparib). A lower ratio of IdU/CldU, which suggests replication fork destabilization and hindered replication, was observed in both PARPi-resistant and PARPi-sensitive cells when treated with CHK1i alone (Fig. 2A). This was not further exacerbated by the addition of olaparib in all PARPi-resistant cell lines except PEO1/OlaJR and PEO4 (fig. S2A). To measure HR repair functionality, RAD51 foci were evaluated (19). Upon olaparib treatment, the number of cells with >5 RAD51 foci increased in all PARPi-resistant cells, attesting to HR restoration in these *BRCA*-mutant cells (Fig. 2B). As previously reported by us and others (20, 21), CHK1i abrogated olaparib-induced RAD51 foci in all cell lines (Fig. 2B and fig. S2B).

DNA damage was assessed by alkaline comet assays, which showed increased comet tail moment with CHK1i monotherapy in all cell lines compared with the control (Fig. 2C). Immunofluorescent staining also showed increased γH2AX foci (DNA damage marker) and pan-γH2AX staining indicating apoptosis (22) in cells treated with CHK1i alone compared with the untreated group (Fig. 2D). We did not observe any increase in either comet tail moment or γH2AX foci in PARPi-resistant cells when treated with CHK1i and olaparib compared with CHK1i alone (fig. S2, C and D). These findings suggest that CHK1i as monotherapy can overcome PARPi resistance in *BRCA*-mutant HGSC by impairing

replication fork dynamics and attenuating HR restoration, leading to DNA damage and lethal replication stress.

CHK1 inhibition reduces tumor growth in PARPi-resistant *BRCA*-mutant HGSC murine models

To confirm the in vitro activity of CHK1i in vivo, we subcutaneously implanted PARPi-sensitive (PEO1) and PARPi-resistant (PEO1/OlaR, PEO1/OlaJR, and de novo PEO4) cells into immunodeficient nonobese diabetic–severe combined immunodeficient gamma (NSG) mice. CHK1i alone significantly reduced tumor growth in all murine models without notable weight loss ($P < 0.001$; Fig. 2E). In contrast, olaparib therapy had little effect on tumor growth in PEO1/OlaR and PEO1/OlaJR models and demonstrated some tumor growth inhibition in de novo PARPi-resistant PEO4 models, although not to the same extent as CHK1i (Fig. 2E). Together, these findings highlight the therapeutic potential of CHK1i in PARPi-resistant HGSC in vivo.

CHK1 inhibition has modest antitumor activity and is well tolerated in patients with PARPi-resistant HGSC with *BRCA* mutation

Because our data indicated the activity of the CHK1i prexasertib in PARPi-resistant *BRCA*-mutant HGSC in vitro and in vivo models, we conducted a proof-of-concept phase 2 clinical trial evaluating prexasertib activity in patients with *BRCA*-mutant recurrent HGSC (NCT02203513). Between February 2015 and July 2019, a total of 22 women were enrolled and received at least one dose of prexasertib (Fig. 3A and fig. S3A). The median age was 56.4 years (range, 35.7 to 74.8 years). About two-thirds of patients (15 of 22) had *BRCA1* mutation, and one-third (7 of 22) had *BRCA2* mutation. Most patients were heavily pretreated with a median of five prior systemic treatments. About 41% of patients (9 of 22) had platinum-sensitive disease and 59% (13 of 22) had secondary platinum-resistant disease. All patients had received platinum-based therapy, and all except one had received previous PARPis. The median duration of PARPi treatment was 9 months (range, 3.5 to 48 months), and the median PARPi-free interval before starting the trial was 4.5 months (range, 1 to 26 months) (Table 1). All patients derived some degree of clinical benefit from previous PARPis, suggesting that PARPi resistance was acquired rather than de novo in this cohort.

Eighteen of 22 patients were evaluable for Response Evaluation Criteria in Solid Tumors (RECIST) v1.1 response (Fig. 3A). Of those, one attained complete response (CR), and another attained partial response (PR), yielding an objective response rate (ORR) of 11% (2 of 18) (Fig. 3B). The patient with CR (41 months of progression-free survival (PFS) and 39 months of duration of response) was the only PARPi-naïve patient in this study, thus resulting in an ORR of 6% (1 of 17) for previously PARPi-treated patients (Fig. 3, B and C, and fig. S3B). Twelve patients (12 of 18, 67%) had stable disease (SD), and four patients (4 of 18, 22%) achieved durable clinical benefit, defined as CR + PR + SD ≥ 6 months (Fig. 3C). There was no difference in clinical benefit by *BRCA1* versus *BRCA2* mutation. Median PFS was 4 months (range, 1.5 to 41 months) among all 18 evaluable patients (Fig. 3C). Four of the initial 22 patients were not evaluable for RECIST response because of withdrawal of consent after one or two doses (two patients); intercurrent illness involving tumor invasion of sigmoid colonic wall in cycle 1 (one patient); and gastric outlet

obstruction by tumor invasion during cycle 1 (one patient), making it too early to assess their response to the treatment. Fourteen patients were assessed for a Gynecologic Cancer Intergroup (GCIG) CA-125 response, meaning a 50% reduction in CA-125 during treatment with confirmation after 4 weeks and pretreatment CA-125 greater than two times the upper limit of normal. Four of the 18 RECIST-evaluable patients were unevaluable for CA-125 response because two did not have at least three serial CA-125 values in the study, and two did not have pretreatment CA-125 greater than two times the upper limit of normal. Six (43%) of these 14 patients had a CA-125 response: one CR (41 months on study, with CA-125 response at 1 month of treatment); four SDs (ranging from 2 to 5 months on study, all with CA-125 response at 1 month of treatment); and one PD (2 months on study, with CA-125 response at 1 month of treatment) (Fig. 3, B and C, and fig. S3C).

All treated patients had at least one-grade treatment-emergent adverse event (AE) (Table 2 and table S3). Prophylactic granulocyte colony-stimulating factor (G-CSF) was not routinely given on cycle 1 day 1 to check for nadir on cycle 1 day 8. Consistent with previous reports (17, 23, 24), the most frequently observed grade 3 or 4 toxicity was neutropenia on cycle 1 day 8 [18 of 22 patients (82%)], and only one patient developed febrile neutropenia. The nadir occurred about 1 week after each dose [median 8 days (range, 8 to 11 days)] and was transient ≤7 days [median 4 days (range, 2 to 13 days)]. G-CSF was given for subsequent treatments to avoid treatment delays or dose reduction in most patients (16 of 18 patients) with grade 3 or 4 neutropenia on day 8 of cycle 1 (Table 2). No patients had dose reductions, and other nonhematologic AEs were relatively mild (table S3). One death occurred during the study off-treatment follow-up period because of the progression of disease (PD) in a patient whose best response was SD. In general, the toxicity profile mirrored that of a previously reported phase 2 cohort of patients with *BRCA*–wild-type HGSC (24). Overall, although prexasertib was largely well tolerated among a heavily pretreated population, its modest ORR, especially among patients previously treated with PARPis, prompted us to investigate possible cross-resistance between PARPis and CHK1i.

BRCA reversion mutation does not confer resistance to CHK1 inhibition

We first questioned whether this limited clinical response to CHK1i in patients with *BRCA*-mutant HGSC previously treated with PARPis correlated with *BRCA* reversion mutations, which have been associated with cross-resistance to PARPis and platinum drugs (25, 26). Pretreatment cell-free DNA (cfDNA) ($n = 18$) and paired tumor tissue samples were available from 15 patients for targeted next-generation sequencing to identify *BRCA* reversion mutations (Fig. 4A). *BRCA* reversion mutations were identified from cfDNA in 33% (6 of 18) of patients and from tissue samples in 33% (5 of 15) of patients (table S4). Overall, *BRCA* reversion mutations did not appear to correlate with the clinical outcome because *BRCA* reversions were seen in three patients with clinical benefit [two SDs (6 and 8 months of PFS) and one PR (17.5 months of PFS)]. All six patients with *BRCA* reversion mutations in cfDNA had the best RECIST response of SD with PFS ranging from 4 to 8 months. Furthermore, all three evaluable patients with the best response of PD, who were resistant to CHK1i treatment at the first restaging scans, did not have *BRCA* reversion mutations. We previously reported a durable clinical benefit rate to prexasertib of 46% in patients with *BRCA*–wild-type HGSC (24), suggesting that CHK1i demonstrates

antitumor activity with functional *BRCA*. Together, these data suggest that *BRCA* reversion mutations are unlikely to confer cross-resistance to CHK1i therapy in PARPi-resistant tumors, although the findings are limited by the relatively small sample size.

Pathways related to high replication stress and low metabolism response are associated with clinical benefit to CHK1i in *BRCA*-mutant HGSC patients

Although sensitivity to CHK1i has been linked to decreased replication fork and DNA repair pathways in *BRCA*–wild-type HGSC cells and tumors (21), the pathways that can predict response to CHK1i in *BRCA*-mutant HGSC remain poorly understood. We thus performed transcriptomic analysis through RNA sequencing (RNA-seq) on pretreatment biopsies obtained from patients deriving clinical benefit (CR + PR + SD ≥ 6 months, $n = 4$) versus those with no clinical benefit (SD + PD < 6 months, $n = 11$) to identify specific pathways related to CHK1i response (Fig. 4A and table S5). Gene set enrichment analysis (GSEA) using gene sets from the Hallmark, Kyoto Encyclopedia of Genes and Genomes (KEGG), and Reactome databases (27) demonstrated the up-regulation of pathways associated with cell cycle progression and DNA repair, including E2F target genes and the G2/M checkpoint, in the clinical benefit group relative to those with no clinical benefit, suggesting that patients deriving clinical benefit have tumors with high dependence on pathways to overcome replication stress (Fig. 4B, left). In contrast, those with no clinical benefit showed the enrichment of pathways related to metabolism (Fig. 4B, right), which coincides with RNA-seq findings on ATR inhibitors (ATRis) in cancers with high replication stress (28). These results also suggest that high replication stress might be associated with clinical benefit to CHK1i, which is supported by what we had observed in PARPi-resistant *BRCA*-mutant cells (Fig. 2A).

High mRNA expression of replication stress and replication fork stabilization is associated with clinical benefit to CHK1i in patients with *BRCA*-mutant HGSC

Studies have shown that replication stress signatures that include genes related to HR and replication fork stability may predict the efficacy of ATR or CHK1is in HGSC (29, 30), although their clinical utility, especially in the *BRCA*-mutant PARPi-resistant HGSC setting, requires further investigation. We asked whether patients expressed specific genes that might indicate replicative stress and replication fork stabilization and whether these genes correlated with response to CHK1i in *BRCA*-mutant PARPi-resistant tumors. Transcriptome profiling did not show any differences in the expression of genes associated with HR repair or PARPi resistance between the clinical benefit versus nonclinical benefit groups, although HR deficiency has been demonstrated to sensitize tumor cells to PARPis and DNA-damaging agents (31) (fig. S4 and table S6). In contrast, the expression of genes involved in replication stress and replication fork stability was increased in patients with clinical benefit (Fig. 5A and table S6). Therefore, we generated a list of 31 genes related to replication fork stabilization [*BLM*, helicase-like transcription factor (*HLTF*), FA complementation group I (*FANCI*), poly(ADP-ribose) glycohydrolase (*PARG*), zinc finger RANBP2-type containing 3 (*ZRANB3*), and TEN1 subunit of CST complex (*TEN1*) found in GSEA analysis)] and 25 known replication stress markers, including *CCNE1*, RB transcriptional corepressor 1 (*RB1*), cyclin-dependent kinase inhibitor 2A (*CDKN2A*), KRAS proto-oncogene, guanosine triphosphatase (*KRAS*), neurofibromin 1 (*NF1*), MYC proto-oncogene, bHLH transcription

factor (*MYC*), erb-b2 receptor tyrosine kinase 2 (*ERBB2*), serine and arginine–rich splicing factor 1 (*SRSF1*), SUV39H1 histone lysine methyltransferase (*SUV39H1*), GINS complex subunit 1 (*GINS1*), phosphoribosyl pyrophosphate synthetase 1 (*PRPS1*), karyopherin subunit alpha 2 (*KPNA2*), aurora kinase B (*AURKB*), transportin 2 (*TNPO2*), origin recognition complex subunit 6 (*ORC6*), cyclin A2 (*CCNA2*), DNA ligase 3 (*LIG3*), metal response element–binding transcription factor 2 (*MTF2*), growth arrest and DNA damage inducible gamma (*GADD45G*), DNA polymerase alpha 1 (*POLA1*), DNA polymerase delta 4 (*POLD4*), DNA polymerase epsilon 4, accessory subunit (*POLE4*), replication factor C subunit 5 (*RFC5*), RecQ-mediated genome instability 1 (*RMI1*), ribonucleotide reductase catalytic subunit M1 (*RRM1*)] in ovarian and other cancers (29, 32) to test which genes might be used as predictive biomarkers for CHK1i response. *BLM* and *CCNE1*, involved in fork stabilization and replication stress, were highly expressed in the clinical benefit group compared with the nonclinical benefit group (Fig. 5, B and C, and table S7). Therefore, we hypothesized that tumors with high dependence on fork stabilization in response to replication stress, as indicated by increased *BLM* and *CCNE1* expression, would be more sensitive to CHK1i treatment in HGSC and that *BLM* could function as a new potential biomarker for clinical benefit to CHK1i.

We also analyzed the mRNA expression and prognostic impact of *BLM* and *CCNE1* using a public Kaplan-Meier plotter ovarian cancer database (33). No difference was found on the basis of the expression of *BLM* (fig. S5A) or *CCNE1* alone (fig. S5B), but high/high coexpression of *BLM* and *CCNE1* in patients showed better PFS compared with those with high *BLM* and low *CCNE1* when treated with topotecan (median PFS 20.63 versus 14.03 months, $P = 0.045$) (fig. S5C), supporting the notion that increased expression of *BLM* and *CCNE1* may serve as biomarkers of predicting the response to DNA replication inhibitors.

BLM overexpression correlates with CHK1i sensitivity in PARPi-resistant *BRCA*-mutant HGSC cells

BLM is a member of the RecQ helicase family, which is critical for replication fork stability by unwinding structures, such as G-quadruplex and Holliday junctions, for DNA replication (34). BLM also helps restart the stalled forks while suppressing the firing of new origins in response to replication stress (35). We thus speculated that increased replication fork stabilization along with replication stress would better predict the sensitivity to CHK1i; furthermore, the role of BLM remains elusive in this phenomenon. To test this idea, we used PARPi-sensitive (PEO1 and UWB) and -resistant *BRCA*-mutant cell lines (PEO1/OlaR, PEO1/OlaJR, and UWB/OlaR) to evaluate the role of BLM because of the paucity of clinical samples. We found that basal BLM protein expression was substantially higher in PARPi-resistant cells relative to their sensitive parental cells (Fig. 6A, top). Moreover, PARPi-resistant cells with high BLM protein expression showed markedly fewer (2.9 to 7.7%) surviving colonies when treated with CHK1i than their parental lines with lower BLM, demonstrating increased sensitivity of the former to CHK1i (Fig. 6A, bottom, and fig. S6A). Furthermore, the sensitivity of both BLM-low and BLM-high cell lines to CHK1i was enhanced when BLM was overexpressed in these cells (Fig. 6B). However, BLM overexpression induced sensitivity to CHK1i that was much greater (4.5- to 42-fold IC_{50}) in PARPi-resistant cells than in their PARPi-sensitive parental cell lines (2.8- and 7.9-fold

in PEO1 and UWB cells, respectively) (Fig. 6C). Cells overexpressing BLM also exhibited similarly enhanced sensitivity to another specific CHK1i, SRA737 (36) (fig. S6B). Together, these data suggest that high BLM abundance in PARPi-resistant cells might predispose them to CHK1i treatment.

Clinical benefit is associated with *CCNE1* amplification

In addition, we examined somatic variants in pretreatment tumors ($n = 15$) using whole-exome sequencing (WES) to identify genetic alterations associated with response to CHK1i. As expected, most tumors (13 of 15) had somatic mutations in *TP53*, consistent with previous reports (2, 37). It has been hypothesized that HGSC with HR deficiency may present a high tumor mutational burden (TMB) and benefit from drugs targeting DNA damage repair (38). However, in our cohort, TMB and somatic variants in HR-related genes were not associated with clinical benefit (fig. S7 and table S8).

As reported previously (39), *CCNE1* amplification was seen in those with clinical benefit (fig. S7). Seven (50%) of 14 evaluable patients had *CCNE1* copy number (CN) gain (CN 2 to 5); three (21%) had CN amplification (CN > 5); and four (29%) had no alterations (Fig. 3B and table S9) (40). It is likely that *CCNE1* amplification in the pretreatment samples was acquired after previous treatment regimens, because *BRCA* mutation and *CCNE1* amplification are generally mutually exclusive (2). All four patients with clinical benefit also harbored *CCNE1* CN gains/amplification and overexpression of its mRNA relative to those without clinical benefit (Figs. 3B and 5C). This finding suggests that tumors with a higher degree of replication stress may demonstrate a more durable response to CHK1i, regardless of *BRCA* mutation status or PARPi resistance. We also examined whether cyclin E1 protein abundance may predict sensitivity to CHK1i. CHK1i sensitivity was not restricted to cells with cyclin E1 protein overexpression (fig. S8), which is consistent with a previous report of prexasertib in HGSC cell lines (18). Additional studies have also suggested that CHK1i sensitivity is not dependent on only cyclin E1 in a subset of cancer cells, including HGSC cells (41, 42). These data further support our finding that increased expression of both *BLM* and *CCNE1*, rather than each independently, may be a better predictor of high replication stress and concomitant sensitivity to DNA repair inhibitors (fig. S5C).

Tumor immune microenvironment shows a positive trend in patients with clinical benefit

Last, we investigated whether a correlation exists between the response of CHK1i and the prevalence of the immunoreactive (IMR) subtype associated with increased immune response, enhanced cytokine expression, and tumor-infiltrating lymphocytes (43–45) in this *BRCA*-mutated HGSC cohort because we previously reported that the tumor immune microenvironment might have a potential predictive role in *BRCA*–wild-type HGSC for CHK1i sensitivity (44). About half (8 of 15) of all evaluable patients showed profiles similar to IMR (fig. S9A), with high activation observed in one patient with CR, although this was not associated with PFS or clinical benefit (fig. S9B). Mesenchymal and proliferative subtypes, characterized by increased stromal components and proliferation markers, respectively (43), were enriched in those without durable clinical benefit, in line with studies suggesting poorer prognosis associated with these subtypes (2, 43). Orthogonally, immunohistochemical analysis of $CD3^+$ T lymphocyte and $CD8^+$ cytotoxic

T cell populations on tissue biopsies of patients with clinical benefit versus those with no clinical benefit showed no difference (fig. S10, A and B and table S10), suggesting that T cell–mediated response in the tumor microenvironment is an unlikely predictive biomarker for determining clinical benefit to CHK1i in the *BRCA*-mutant setting.

DISCUSSION

There is an urgent unmet need for therapeutic agents and relevant biomarkers to predict response in PARPi-resistant HGSC. In this study, high-throughput drug screens of both *BRCA*-mutant and *BRCA*-restored PARPi-resistant HGSC cell lines revealed high scores for agents that target replication fork stability and DNA replication, with the CHK1i prexasertib ranked high on the list. Prexasertib has shown clinical benefit previously in the treatment of patients with recurrent *BRCA*–wild-type HGSC (24) and in preclinical models of PARPi-resistant HGSC (18). Here, we also observed considerable antitumor activity of CHK1i in PARPi-resistant HGSC cell lines irrespective of *BRCA* functional status. Although our study demonstrated durable single-agent activity of CHK1i in a proportion of this cohort of PARPi-pretreated patients with HGSC and *BRCA* mutation, the results suggest that a biomarker approach that can improve the ORR in response to CHK1i is needed.

Currently, there is no clearly defined replication stress biomarker to predict the response of CHK1i in the *BRCA*-mutant HGSC setting, although *CCNE1* overexpression or CN gain has been studied as a potential biomarker in HGSC for CHK1i sensitivity (6, 24). The EVOLVE study (39) and others (46, 47) have found that *CCNE1* amplification or overexpression induces chemoresistance in ovarian cancer. However, recent clinical studies have shown that *CCNE1* overexpression or CN gain alone might not predict the sensitivity to cell cycle checkpoint blockade (30, 48). In addition, a recent study by Konstantinopoulos *et al.* (29) identified replication stress signatures for the ATRi berzosertib and gemcitabine sensitivity in patients with HGSC. In this study, patients with HGSC with high replication stress benefited from gemcitabine alone, whereas those with low replication stress tumors benefited from the addition of berzosertib to gemcitabine (29). However, in our cohort, the replication stress signatures, including *RB1* two-copy loss, *CDKN2A* two-copy loss, *KRAS* amplification, *ERBB2* amplification, *MYC* amplification, *NF1* mutations, and *MYCL1* amplification (29), were not associated with clinical benefit to CHK1i (fig. S7 and table S9), suggesting that further investigation is required.

In the current study, we found that mRNA overexpression of the RecQ helicase *BLM*, along with replication stress marker *CCNE1*, was associated with increased clinical benefit to CHK1i in patients with HGSC with *BRCA* mutation. Mechanistically, BLM is one of the key responders of stalled replication forks during replication stress (49). Preclinical studies have identified the up-regulation of BLM or BLM-positive ultrafine bridges in *CCNE1*-overexpressing primary human fallopian tube epithelial cells (50) and *RB1*-deficient osteoblastoma cells (51). Similarly, increased recruitment of BLM on stalled replication forks was observed in cells with high protein expression of replication protein A and single-stranded DNA (52), suggesting BLM's critical function in replication fork stability, particularly under high replication stress. Also, *BLM* CN gain or increased *BLM* mRNA expression was shown in patients with platinum-sensitive triple-negative breast

cancer, suggesting its potential use in the clinic (35). Together, these reports along with our findings suggest the potential of BLM as a predictive biomarker for drugs targeting replication fork stabilization.

Although several PARPi resistance mechanisms have been described in preclinical models, clinical data are relatively scarce and mostly confirm the prevalence of reversion mutations as a primary driver of PARPi resistance (4, 25, 53). Hence, it is noteworthy that BRCA restoration had little correlation with the sensitivity to prior PARPi or platinum-based therapy and did not exclude a benefit from CHK1i in our cohort. A transcriptomic signature of replication stress has been reported as a predictive biomarker for ATR and WEE1 inhibitors in patient-derived pancreatic cancer cells and xenografts, in which response, similar to our findings, was not associated with HR deficiency (54). Thus, the use of replication stress and replication fork biomarkers might be more edifying toward predicting CHK1i and other cell cycle checkpoint inhibitors' response (such as ATR and WEE1 inhibitors) when *BRCA* reversion mutations are factored in. Another factor that might be considered in this scenario is the immune milieu in the tumor microenvironment that has been previously shown by us and others (44, 55, 56) to be associated with clinical benefit to prexasertib in *BRCA*–wild-type HGSC. However, we did not observe the same association in the *BRCA*-mutant setting, further highlighting the complex molecular dynamics of PARPi resistance and CHK1i sensitivity.

Limitations of our study include the small size of the clinical trial and the progressive nature of PARPi resistance development. There was only one patient who was PARPi naïve, limiting the comparisons that could be made among PARPi-resistant and PARPi-sensitive subgroups in this cohort. Furthermore, the results of the present study in comparison with those of other clinical trials must be interpreted with caution given the lack of a standardized definition of clinical PARPi resistance, which we defined as progression on a previous PARPi at any time in the treatment life cycle after having an initial response to PARPi. One way to address these challenges would be by increasing the number of clinical trials in the PARPi-resistant patient population with mandatory biopsies on enrollment along with a collection of archival tissues because this will be key to evaluate a dynamic measure of tumor replication stress status to provide the best treatment options. Also, all biomarker analyses are exploratory and hypothesis-generating in nature and warrant validation in a larger, prospective setting. In the current study, we were unable to examine whether protein overexpression of BLM or cyclin E1 in clinical samples, in addition to mRNA up-regulation, correlates with clinical benefit to CHK1i because of the paucity of fresh core biopsy samples. This should be further investigated in the *BRCA*-mutant HGSC setting because cyclin E1 protein overexpression by immunohistochemistry staining has been associated with a higher ORR in platinum-resistant HGSC to the WEE1 inhibitor adavosertib (57). We contend that patients with high mRNA expression of replication stress along with replication fork-related biomarkers should be considered for CHK1i-based therapy.

In summary, we demonstrated the therapeutic potential of CHK1i in a subgroup of *BRCA*-mutant HGSC, both in the preclinical and clinical settings, and reported that tumors with high dependence on replication fork stabilization may help identify patients for CHK1i irrespective of PARPi resistance, warranting further prospective validation. Ultimately,

our comprehensive molecular assessment of pretreatment tumors will help to guide the development of more personalized treatment regimens and improve patient stratification in HGSC with *BRCA* mutation.

MATERIALS AND METHODS

Study design

The aim of this study was to investigate the clinical activity of CHK1i prexasertib in PARPi-resistant *BRCA*-mutant HGSC and to identify potential biomarkers for CHK1i response. Fresh tumor biopsy and blood samples were collected from *BRCA*-mutant HGSC cohort patients from the single-arm, open-label phase 2 basket study of prexasertib at the National Cancer Institute (NCI) (NCT02203513). All patients provided written informed consent before enrollment. The study was conducted in accordance with ethical principles founded in the Declaration of Helsinki. The trial was approved by the Institutional Review Board of the Center for Cancer Research (CCR), NCI, USA. All eligible patients received intravenous prexasertib monotherapy at 105 mg/m^2 over 1 hour every 2 weeks in 4-week cycles. The primary endpoint was investigator-assessed ORR (CR + PR) according to RECIST v1.1. Secondary endpoints included safety and toxicity evaluation per Common Terminology Criteria for Adverse Events (CTCAE) v4.0 and PFS, defined as the time from enrollment until the first documented disease progression according to RECIST v1.1 or death resulting from any cause. The full study design of the clinical trial is described in Supplementary Materials and Methods.

Preclinical experiments

Cell lines—The UWB (*BRCA1* mutation 2594delC) cell line was purchased from American Type Culture Collection (#CRL-2945). The PEO1 (*BRCA2* mutation 5193C>G; #10032308–1VL) and PEO4 (*BRCA2* reversion mutation 5193C>T; #10032309–1VL) cell lines were purchased from Sigma-Aldrich. The PARPi-resistant PEO1/OlaJR cell line was developed from parental PEO1 by culturing cells with olaparib from 5 to 40 μM over 3 to 4 months (13). Similarly, PARPi-resistant UWB/OlaR cells were developed from parental UWB by exposing them to olaparib from 0.5 to 20 μM over 12 months. Another PARPi-resistant PEO1/OlaR cell line was a gift from the laboratory of B. Bitler (16). PEO1 and UWB cells were grown in RPMI1640 medium with (+) L-glutamine supplemented with 10% fetal bovine serum, insulin (0.01 mg/ml), and 1% penicillin/streptomycin. PARPi-resistant cell lines were routinely maintained at 5 μM (PEO1/OlaR) or 20 μM olaparib (UWB/OlaR and PEO1/OlaJR). Cells were cultured without olaparib for at least 3 days before being used for the following experiments.

Chemical preparation—For in vitro assays, olaparib (#S1060), prexasertib (#S7178), and SRA737 (CCT245737, #S8253) were purchased from Selleck Chemicals. Olaparib (100 μM) and 10 μM prexasertib and SRA737 were prepared as stocks in dimethyl sulfoxide (DMSO; #S-002-M, Sigma-Aldrich). All drugs were stored in aliquots at −80°C until use. For in vivo studies, prexasertib mesylate hydrate (prexasertib; #1234015–57-6, InvivoChem LLC) was prepared in 20% CAPTISOL (CyDex Pharmaceuticals Inc.,), whereas olaparib (#V300, InvivoChem LLC) was formulated in phosphate-buffered saline (PBS) containing

10% DMSO and 10% (w/v) 2-hydroxy-propyl-β-cyclodextrin as described previously (18, 58).

High-throughput single-agent drug screening—High-throughput single-agent drug screening was performed as previously reported (15). Briefly, 20 nl of MIPE 5.0 compounds were acoustically dispensed by Echo Acoustic Liquid Handler (Beckman Coulter Life Sciences) into 1536-well white tissue culture–treated plates. Each compound was plated at an 11-point concentration range with 1:3 dilution. Bortezomib, a proteasome inhibitor (final concentration, 20 μM), was used as a positive control for cell cytotoxicity. PEO1, PEO4, and PEO1/OlaR were trypsinized and dispensed in 5 μl of growth medium using a Multi-drop Combi dispenser at a density of 600 cells per well to allow for compounds to be present during the exponential growth phase. Plates were incubated for 96 hours at standard incubator conditions and covered by a stainless steel gasketed lid to prevent evaporation. Three microliters of CellTiter-Glo (Promega) were added to each well, and plates were incubated at room temperature for 15 min with a stainless steel lid in place. Luminescence readings were taken using PHERAstar (BMG Labtech). Compound dose-response curves were normalized to DMSO and empty well controls on each plate. The average Z-AUC was calculated to determine inactive and active drug responses. Drugs with average Z-AUC values less than −1.0 in PARPi-sensitive and -resistant HGSC cell lines in the MIPE 5.0 dataset were defined as hits (15), indicating active drugs.

Cell proliferation assays: XTT and colony-forming assays—Cell survival ability was evaluated in response to prexasertib and olaparib. For short-term cell survival, a 2,3-bis-(2-methoxy-4-nitro-5-sulfophenyl)-2H-tetrazolium-5-carboxanilide (XTT) assay (#X6493, Thermo Fisher Scientific) was performed. Two thousand cells per well were seeded in 96-well plates and treated with clinically attainable concentrations of prexasertib [0.125 to 100 nM (17)] and olaparib [2.5 to 50 μM (59)] for 72 hours. The plates were measured by Synergy HTX Multimode Microplate Reader with Gen5 software (BioTek Instruments). IC_{50} values were calculated using GraphPad Prism v7.1 (GraphPad Software). The CI values were evaluated by CompuSyn software (ComboSyn Inc). CI values less than 1 indicate synergism, whereas CI values greater than 1 indicate antagonism (60).

For long-term cell survival with prexasertib and or olaparib treatment, a colony-forming assay was used. Five thousand cells were seeded in 24-well plates and treated with prexasertib (0.5 nM for UWB and 5 nM for all other cell lines), olaparib (10 μM), or both. Media and drugs were changed every 3 days for 12 to 15 days. Fixed colonies were stained with 0.01% (w/v) crystal violet in PBS. Colony images were scanned, and quantification of colony area percentage was done using ImageJ software (National Institutes of Health, NIH).

Immunoblotting—Active CHK1 (pCHK1-S296) and total CHK1 were measured to evaluate the target effects of CHK1i. Cells were treated with prexasertib (0.5 nM for UWB and 5 nM for all other cell lines). After 48-hour treatment, cells were collected for protein extraction and subjected to immunoblotting. Blots were visualized using the LI-COR Odyssey Imaging System. BLM (#2742), CHK1 (#2360), pCHK1-S296 (#2349), enhanced chemiluminescence (ECL) goat antimouse immunoglobulin G (IgG) horseradish peroxidase

(HRP) (#7076), and ECL goat anti-rabbit IgG HRP (#7074) antibodies were purchased from Cell Signaling Technology. Cyclin E1 antibody (#ab74276) was purchased from Abcam.

DNA fiber assay—DNA fiber assay was performed as described (58). Cells were labeled with 60 μM CldU (#I7125, Sigma-Aldrich) for 20 min, washed quickly and exposed to 500 μM IdU (C6891, Sigma-Aldrich) for 10 min, and then treated with or without prexasertib (20 nM) or olaparib (20 μM) for another 2 hours. Cells were collected and lysed with lysis buffer [1% SDS, 100 mM tris-HCl (pH 7.4), and 50 mM EDTA]. Labeled DNAs with CldU and IdU were stained with mouse anti-IdU primary antibody (1:250; #NBP2–44056, Novus Biological) and rat anti-CldU primary (1:200; #NB500–169, Novus Biological), respectively. Anti-rat Alexa Fluor 488 (1:250; #A-11006, Thermo Fisher Scientific) and anti-mouse Alexa Fluor 594 (1:250; #A-11005, Thermo Fisher Scientific) were used for secondary antibodies. Images were captured with a Zeiss LSM 780 confocal microscope. Fiber length was measured using ImageJ software (NIH).

Assays for detecting DNA damage and HR repair status: Alkaline comet assay and immunofluorescence staining of γH2AX and RAD51 foci—For DNA damage endpoints, DNA fragmentations and immunofluorescence staining of γH2AX foci formation were studied. Cells were treated with prexasertib (0.5 nM for UWB and 5 nM for all other cell lines), olaparib (10 μM), or both for 48 hours. DNA fragmentations were analyzed by alkaline comet assay according to the manufacturer's instructions (Trevigen). The mean tail moment from three independent experiments (each experiment scored at least 100 cells per treatment) was calculated as an index of DNA damage by using CometScore Pro (TriTek Corporation). For γH2AX foci formation, the cells were grown on Falcon Chambered Cell Culture Slides (Corning Inc). After drug treatment for 48 hours, cells were fixed in 4% paraformaldehyde (PFA) for 10 min, permeabilized with 0.25% Triton-X 100, and blocked with 1% bovine serum albumin in PBS for another 10 min. For RAD51 foci formation, cells were fixed in 3.7% PFA containing 2% sucrose and 0.5% Triton X on ice as previously described (61). All images were collected with an LSM 780 confocal microscope with a 63×/1.4 oil immersion objective. The number of γH2AX foci per nucleus was quantified by ImageJ software. Cells with 5 to 15 γH2AX foci per nucleus and pan-nuclear γH2AX staining were counted (20). Cells with >5 RAD51 foci per nucleus were counted as RAD51-positive cells (61).

BLM overexpression experiments—The GFP-BLM vector was a gift from N. Ellis (#80070, Addgene) (62). Cells were seeded and transfected with GFP-BLM (100 ng) or GFP empty vector in 96-well plates at a 3:1 FuGENE HD Transfection Reagent:DNA ratio according to the manufacturer's instruction (#E2311, Promega) for 48 hours. Cells were then treated with prexasertib for another 48 hours and subjected to cell proliferation assays.

Animal study—Xenograft murine models were used to evaluate the efficacy of prexasertib and olaparib in vivo. All animal procedures reported in this study that were performed by NCI-CCR–affiliated staff were approved by the NCI Animal Care and Use Committee (ACUC) and in accordance with federal regulatory requirements and standards. All components of the intramural NIH ACUC program are accredited by the Association for

Assessment and Accreditation of Laboratory Animal Care International. A total of 5×10^6 cells were suspended in 50 μl of cold PBS and mixed with 50 μl of Matrigel. A total of 100 μl of cell mixture were subcutaneously injected into 6-week-old female NSG mice (NCI). The volume of a tumor was measured once per week according to the formula $V = ½ (\text{length} \times \text{width}^2)$. When tumors reached 50 mm^3, mice were randomized into three groups ($n = 5$ per group). Mice received vehicle or prexasertib (8 mg/kg) by intraperitoneal (ip) injection twice daily (BID) for 3 days, followed by 4 days of no treatment for a total of 3 weeks (58). For combination studies, two study arms were added, and mice received olaparib (100 mg/kg) orally once daily for 5 days, followed by 2 days of no treatment (18) with or without prexasertib (8 mg/kg, ip) BID for 3 days, followed by 4 days of no treatment for 3 weeks. All mice were euthanized at the end of treatments.

Clinical trial

The full study methodology is described in Supplementary Materials and Methods. Briefly, eligible patients received intravenous prexasertib monotherapy at 105 mg/m^2 over 1 hour every 2 weeks in 4-week cycles (fig. S3A). Clinical response per RECIST v1.1 was assessed by the investigator every two cycles by computed tomography (CT) imaging or magnetic resonance imaging. Serum CA-125 response was investigated every cycle as a post hoc exploratory endpoint and was defined as a 50% reduction during treatment with confirmation after 4 weeks according to GCIG criteria (63).

Patients were evaluated for toxicity per CTCAE v4.0. AEs were assessed before administration of the study drug on days 1 and 15 of cycle one and before the start of every subsequent cycle. Transient (lasting ≤7 days) grade 3 or 4 neutropenia without fever or febrile neutropenia on cycle 1 without growth factor support did not require dose reduction or discontinuation of treatment. Patients received treatment until PD, intercurrent illness, AEs not recovering to ≤grade 1 within a 3-week period, or patient withdrawal of consent. Treatment interruptions of up to 7 days were permitted because of holidays, inclement weather preventing clinic attendance, toxic effects, or similar reasons.

Correlative studies

For post hoc correlative studies, we collected pretreatment CT- or ultrasound-guided fresh-frozen core biopsies ($n = 15$) and blood samples ($n = 18$) at baseline. Three patients had pretreatment biopsies canceled because of safety reasons. Prespecified post hoc exploratory objectives were the investigation of potentially predictive biomarkers of response to CHK1i in tumor and blood samples.

BRCA reversion mutation assay—cfDNA sequencing libraries were prepared from 5 to 10 ng of cfDNA input using the KAPA HyperPrep kit (Roche Sequencing and Life Science). Samples were individually barcoded using xGen UDI-UMI adapters (Integrated DNA Technologies) and then pooled before multiplexed hybridization capture using xGen NGS Hybridization Capture for NGS target enrichment (Integrated DNA Technologies) targeting 200 kb of genomic territory derived from assorted coding segments of 68 cancer-associated genes. Samples were subsequently amplified, purified using AMPure beads

(Beckman Coulter Life Sciences), and quantified before sequencing on the Illumina NextSeq 500.

Samples were sequenced to no more than 50 million read pairs. Bioinformatics was performed by the University of Washington NGS Analytics Laboratory. After demultiplexing and alignment, fgbio (Fulcrum Genomics) was used to group reads by the unique molecular indices applied during adapter ligation before the polymerase chain reaction. Families with fewer than five reads and those where greater than 5% of bases were identified as erroneous were discarded; the rest were collapsed into a single consensus sequence for each family, thereby reducing background noise due to sequencer error. In the postprocessed sequence, bases where consensus could not be determined or where more than 10% of contributing reads did not support the consensus were masked to N. Collapsed families with more than 10% of their bases masked were also discarded. Samples were then realigned, and variants were called using VarDict (AstraZeneca-NGS). Alternate alleles that were supported by at least one read (with a base quality score of >10) and with variant allele frequencies of >0.001% were emitted to the initial variant call format, which was filtered to a finalized list of mutations using custom filtration parameters. Large insertions and deletions were detected by manual inspection of regions adjacent to known germline alterations using Integrative Genomics Viewer (Broad Institute).

RNA-seq and WES—RNA-seq and WES were performed using a HiSeq 3000 sequencing system (Illumina) at the NCI CCR Sequencing Facility, Frederick National Laboratory for Cancer Research, as detailed previously (44). More specific details are provided in Supplementary Materials and Methods.

Statistical analyses

Preclinical studies—Three independent biological replicates were performed in all experiments. Investigators were blinded during data collection and analysis. Data were analyzed using a one-way analysis of variance (ANOVA) test and are shown as means ± SEM. The Pearson's correlation coefficient was used to analyze the correlation between basal BLM protein expression and colony-forming ability in cells with CHK1i treatment. All differences were considered statistically significant if $P < 0.05$. All statistical analyses were done using GraphPad Prism v7.1 (GraphPad Software).

Clinical trial—The sample size was selected using Simon's two-stage phase 2 design to rule out an unacceptably low 5% ORR in favor of an improved 25% ORR, with $\alpha = 0.10$ and $\beta = 0.10$. These parameters were chosen to minimize the number of women exposed to a potentially inactive agent and to target a sufficiently high ORR to support moving into a definitive trial should this trial be positive. A response in 1 of the first 9 patients sufficed to move to the second stage of accrual, adding another 15 patients for a total of 24 patients. The regimen would be considered sufficiently interesting if ≥3 of 24 patients (12.5%) had a CR or PR, but the study was closed after enrolling 22 patients because of slow accrual. The null hypothesis of 5% was selected to accommodate the inclusion of heavily pretreated patients based on the findings of the Gynecologic Oncology Group 0126 series of cancer trials, in which the proportion of patients with response was 3 to 4%

(64). Under the null hypothesis, the probability of early termination was 63.0%. PFS was estimated using the Kaplan-Meier method beginning at the on-study date and continuing until progression or death without progression. Safety evaluation was based on all enrolled patients. Descriptive statistics were used to summarize the number and types of AEs. Patients considered non-evaluable had either no post-baseline CT scan or discontinued after less than 8 weeks without documented progression.

All statistical tests for correlative studies used a two-sided significance level of 0.05 and are reported without adjustment for multiple comparisons because of the small study cohort and exploratory nature of this analysis. Statistical tests for correlative studies used a two-sided significance level of 0.05. For gene expression profile analysis, we used the limma VOOM method followed by adjusting with a Benjamini-Hochberg false discovery rate cutoff of <10% [adjusted P value (q) < 0.1 indicates significance] for multiple hypothesis testing (65). This method allows for different mRNA levels of variability between genes and between samples and makes statistical conclusions more reliable (65–67).

Supplementary Material

Refer to Web version on PubMed Central for supplementary material.

Acknowledgments:

We thank C. Annunziata, M. Gomez, N. Houston, E. Kohn, S. Lipkowitz, E. Villanueva, and A. Zimmer for contributions in clinic; S. Steinberg for assistance in statistical analysis of the clinical trial; and N. Nair for consultation on gene expression profile analysis. Eli Lilly supplied prexasertib to the NCI CCR under a cooperative research and development agreement.

Funding:

This work was supported by the Intramural Research Program of the Center for CCR of NCI, NIH (ZIA BC011525, to J.-M.L.); NIH Medical Research Scholars Program, a public-private partnership supported jointly by the NIH and contributions to the Foundation for the NIH from the Doris Duke Charitable Foundation, Genentech, the American Association for Dental Research, and the Colgate-Palmolive Company (to N.G.); the Intramural Research Program grant of the National Center for Advancing Translational Sciences and the CCR of NCI, NIH (FY21-NCI-01, to J.-M.L., T.-T.H., and K.C.-C.C.); and the Department of Defense Investigator-initiated Research Award (OC160355, to E.M.S.).

REFERENCES AND NOTES

1. Siegel RL, Miller KD, Fuchs HE, Jemal A, Cancer Statistics, 2021. CA Cancer J. Clin 71, 7–33 (2021). [PubMed: 33433946]
2. Cancer Genome Atlas Research Network, Integrated genomic analyses of ovarian carcinoma. Nature 474, 609–615 (2011). [PubMed: 21720365]
3. Banerjee S, Gonzalez-Martin A, Harter P, Lorusso D, Moore KN, Oaknin A, Ray-Coquard I, First-line PARP inhibitors in ovarian cancer: Summary of an ESMO Open - Cancer Horizons round-table discussion. ESMO Open 5, e001110 (2020).
4. Dias MP, Moser SC, Ganesan S, Jonkers J, Understanding and overcoming resistance to PARP inhibitors in cancer therapy. Nat. Rev. Clin. Oncol 18, 773–791 (2021). [PubMed: 34285417]
5. Konstantinopoulos PA, Lheureux S, Moore KN, PARP inhibitors for ovarian cancer: Current indications, future combinations, and novel assets in development to target DNA damage repair. Am. Soc. Clin. Oncol. Educ. Book 2020, e116–e131 (2020).

6. Gupta N, Huang T, Horibata S, Lee J, Cell cycle checkpoints and beyond: Exploiting the ATR/CHK1/WEE1 pathway for the treatment of PARP inhibitor–resistant cancer. Pharmacol. Res 178, 106162 (2022).

7. Techer H, Koundrioukoff S, Carignon S, Wilhelm T, Millot GA, Lopez BS, Brison O, Debatisse M, Signaling from Mus81-Eme2-dependent DNA damage elicited by Chk1 deficiency modulates replication fork speed and origin usage. Cell Rep. 14, 1114–1127 (2016). [PubMed: 26804904]

8. Couch FB, Bansbach CE, Driscoll R, Luzwick JW, Glick GG, Betous R, Carroll CM, Jung SY, Qin J, Cimprich KA, Cortez D, ATR phosphorylates SMARCAL1 to prevent replication fork collapse. Genes Dev. 27, 1610–1623 (2013). [PubMed: 23873943]

9. Lossaint G, Larroque M, Ribeyre C, Bec N, Larroque C, Decaillet C, Gari K, Constantinou A, FANCD2 binds MCM proteins and controls replisome function upon activation of s phase checkpoint signaling. Mol. Cell 51, 678–690 (2013). [PubMed: 23993743]

10. Kim H, Xu H, George E, Hallberg D, Kumar S, Jagannathan V, Medvedev S, Kinose Y, Devins K, Verma P, Ly K, Wang Y, Greenberg RA, Schwartz L, Johnson N, Scharpf RB, Mills GB, Zhang R, Velculescu VE, Brown EJ, Simpkins F, Combining PARP with ATR inhibition overcomes PARP inhibitor and platinum resistance in ovarian cancer models. Nat. Commun 11, 3726 (2020). [PubMed: 32709856]

11. Kim H, George E, Ragland R, Rafail S, Zhang R, Krepler C, Morgan M, Herlyn M, Brown E, Simpkins F, Targeting the ATR/CHK1 axis with PARP inhibition results in tumor regression in BRCA-mutant ovarian cancer models. Clin. Cancer Res 23, 3097–3108 (2017). [PubMed: 27993965]

12. Yap TA, O'Carrigan B, Penney MS, Lim JS, Brown JS, de Miguel Luken MJ, Tunariu N, Perez-Lopez R, Rodrigues DN, Riisnaes R, Figueiredo I, Carreira S, Hare B, McDermott K, Khalique S, Williamson CT, Natrajan R, Pettitt SJ, Lord CJ, Banerji U, Pollard J, Lopez J, de Bono JS, Phase I trial of first-in-class ATR inhibitor M6620 (VX-970) as monotherapy or in combination with carboplatin in patients with advanced solid tumors. J. Clin. Oncol 38, 3195–3204 (2020). [PubMed: 32568634]

13. Huang TT, Burkett SS, Tandon M, Yamamoto TM, Gupta N, Bitler BG, Lee JM, Nair JR, Distinct roles of treatment schemes and BRCA2 on the restoration of homologous recombination DNA repair and PARP inhibitor resistance in ovarian cancer. Oncogene 41, 5020–5031 (2022). [PubMed: 36224341]

14. Kaur E, Agrawal R, Sengupta S, Functions of BLM helicase in cells: Is it acting like a doubleedged sword? Front. Genet 12, 634789 (2021).

15. Lin GL, Wilson KM, Ceribelli M, Stanton BZ, Woo PJ, Kreimer S, Qin EY, Zhang X, Lennon J, Nagaraja S, Morris PJ, Quezada M, Gillespie SM, Duveau DY, Michalowski AM, Shinn P, Guha R, Ferrer M, Klumpp-Thomas C, Michael S, McKnight C, Minhas P, Itkin Z, Raabe EH, Chen L, Ghanem R, Geraghty AC, Ni L, Andreasson KI, Vitanza NA, Warren KE, Thomas CJ, Monje M, Therapeutic strategies for diffuse midline glioma from high-throughput combination drug screening. Sci. Transl. Med 11, eaaw0064 (2019).

16. Yamamoto TM, McMellen A, Watson ZL, Aguilera J, Ferguson R, Nurmemmedov E, Thakar T, Moldovan GL, Kim H, Cittelly DM, Joglar AM, Brennecke EP, Wilson H, Behbakht K, Sikora MJ, Bitler BG, Activation of Wnt signaling promotes olaparib resistant ovarian cancer. Mol. Carcinog 58, 1770–1782 (2019). [PubMed: 31219654]

17. Hong D, Infante J, Janku F, Jones S, Nguyen LM, Burris H, Naing A, Bauer TM, Piha-Paul S, Johnson FM, Kurzrock R, Golden L, Hynes S, Lin J, Lin AB, Bendell J, Phase I study of LY2606368, a checkpoint kinase 1 inhibitor, in patients with advanced cancer. J. Clin. Oncol 34, 1764–1771 (2016). [PubMed: 27044938]

18. Parmar K, Kochupurakkal BS, Lazaro J-B, Wang ZC, Palakurthi S, Kirschmeier PT, Yang C, Sambel LA, Färkkilä A, Reznichenko E, Reavis HD, Dunn CE, Zou L, Do KT, Konstantinopoulos PA, Matulonis UA, Liu JF, D'Andrea AD, Shapiro GI, The CHK1 inhibitor prexasertib exhibits monotherapy activity in high-grade serous ovarian cancer models and sensitizes to PARP inhibition. Clin. Cancer Res 25, 6127–6140 (2019). [PubMed: 31409614]

19. Cruz C, Castroviejo-Bermejo M, Gutiérrez-Enríquez S, Llop-Guevara A, Ibrahim YH, Gris-Oliver A, Bonache S, Morancho B, Bruna A, Rueda OM, Lai Z, Polanska UM, Jones GN, Kristel P, de Bustos L, Guzman M, Rodríguez O, Grueso J, Montalban G, Caratú G, Mancuso F, Fasani

R, Jiménez J, Howat WJ, Dougherty B, Vivancos A, Nuciforo P, Serres-Créixams X, Rubio IT, Oaknin A, Cadogan E, Barrett JC, Caldas C, Baselga J, Saura C, Cortés J, Arribas J, Jonkers J, Díez O, O'Connor MJ, Balmaña J, Serra V, RAD51 foci as a functional biomarker of homologous recombination repair and PARP inhibitor resistance in germline BRCA-mutated breast cancer. Ann. Oncol 29, 1203–1210 (2018). [PubMed: 29635390]

20. Brill E, Yokoyama T, Nair J, Yu M, Ahn YR, Lee JM, Prexasertib, a cell cycle checkpoint kinases 1 and 2 inhibitor, increases in vitro toxicity of PARP inhibition by preventing Rad51 foci formation in BRCA wild type high-grade serous ovarian cancer. Oncotarget 8, 111026–111040 (2017).
21. Nair J, Huang TT, Murai J, Haynes B, Steeg PS, Pommier Y, Lee JM, Resistance to the CHK1 inhibitor prexasertib involves functionally distinct CHK1 activities in BRCA wild-type ovarian cancer. Oncogene 39, 5520–5535 (2020). [PubMed: 32647134]
22. de Feraudy S, Revet I, Bezrookove V, Feeney L, Cleaver JE, A minority of foci or pannuclear apoptotic staining of gammaH2AX in the S phase after UV damage contain DNA double-strand breaks. Proc. Natl. Acad. Sci. U.S.A 107, 6870–6875 (2010). [PubMed: 20351298]
23. Gatti-Mays ME, Karzai FH, Soltani SN, Zimmer A, Green JE, Lee MJ, Trepel JB, Yuno A, Lipkowitz S, Nair J, McCoy A, Lee JM, A phase II single arm pilot study of the CHK1 inhibitor prexasertib (LY2606368) in BRCA wild-type, advanced triple-negative breast cancer. Oncologist 25, 1013–e1824 (2020). [PubMed: 32510664]
24. Lee JM, Nair J, Zimmer A, Lipkowitz S, Annunziata CM, Merino MJ, Swisher EM, Harrell MI, Trepel JB, Lee MJ, Bagheri MH, Botesteanu DA, Steinberg SM, Minasian L, Ekwede I, Kohn EC, Prexasertib, a cell cycle checkpoint kinase 1 and 2 inhibitor, in BRCA wild-type recurrent high-grade serous ovarian cancer: A first-in-class proof-of-concept phase 2 study. Lancet Oncol. 19, 207–215 (2018). [PubMed: 29361470]
25. McMullen M, Karakasis K, Madariaga A, Oza AM, Overcoming platinum and PARP-inhibitor resistance in ovarian cancer. Cancers (Basel) 12, 1607 (2020). [PubMed: 32560564]
26. Lin KK, Harrell MI, Oza AM, Oaknin A, Ray-Coquard I, Tinker AV, Helman E, Radke MR, Say C, Vo LT, Mann E, Isaacson JD, Maloney L, O'Malley DM, Chambers SK, Kaufmann SH, Scott CL, Konecny GE, Coleman RL, Sun JX, Giordano H, Brenton JD, Harding TC, McNeish IA, Swisher EM, BRCA reversion mutations in circulating tumor DNA predict primary and acquired resistance to the PARP inhibitor rucaparib in high-grade ovarian carcinoma. Cancer Discov. 9, 210–219 (2019). [PubMed: 30425037]
27. Subramanian A, Tamayo P, Mootha VK, Mukherjee S, Ebert BL, Gillette MA, Paulovich A, Pomeroy SL, Golub TR, Lander ES, Mesirov JP, Gene set enrichment analysis: A knowledge-based approach for interpreting genome-wide expression profiles. Proc. Natl. Acad. Sci. U.S.A 102, 15545–15550 (2005). [PubMed: 16199517]
28. Thomas A, Takahashi N, Rajapakse VN, Zhang X, Sun Y, Ceribelli M, Wilson KM, Zhang Y, Beck E, Sciuto L, Nichols S, Elenbaas B, Puc J, Dahmen H, Zimmermann A, Varonin J, Schultz CW, Kim S, Shimellis H, Desai P, Klumpp-Thomas C, Chen L, Travers J, McKnight C, Michael S, Itkin Z, Lee S, Yuno A, Lee MJ, Redon CE, Kindrick JD, Peer CJ, Wei JS, Aladjem MI, Figg WD, Steinberg SM, Trepel JB, Zenke FT, Pommier Y, Khan J, Thomas CJ, Therapeutic targeting of ATR yields durable regressions in small cell lung cancers with high replication stress. Cancer Cell 39, 566–579.e7 (2021). [PubMed: 33848478]
29. Konstantinopoulos PA, da Costa A, Gulhan D, Lee EK, Cheng SC, Hendrickson AEW, Kochupurakkal B, Kolin DL, Kohn EC, Liu JF, Stover EH, Curtis J, Tayob N, Polak M, Chowdhury D, Matulonis UA, Farkkila A, D'Andrea AD, Shapiro GI, A replication stress biomarker is associated with response to gemcitabine versus combined gemcitabine and ATR inhibitor therapy in ovarian cancer. Nat. Commun 12, 5574 (2021). [PubMed: 34552099]
30. Hill SJ, Decker B, Roberts EA, Horowitz NS, Muto MG, Worley MJ Jr., Feltmate CM, Nucci MR, Swisher EM, Nguyen H, Yang C, Morizane R, Kochupurakkal BS, Do KT, Konstantinopoulos PA, Liu JF, Bonventre JV, Matulonis UA, Shapiro GI, Berkowitz RS, Crum CP, D'Andrea AD, Prediction of DNA repair inhibitor response in short-term patient-derived ovarian cancer organoids. Cancer Discov. 8, 1404–1421 (2018). [PubMed: 30213835]
31. Cleary JM, Aguirre AJ, Shapiro GI, D'Andrea AD, Biomarker-guided development of DNA repair inhibitors. Mol. Cell 78, 1070–1085 (2020). [PubMed: 32459988]

32. Jo U, Senatorov IS, Zimmermann A, Saha LK, Murai Y, Kim SH, Rajapakse VN, Elloumi F, Takahashi N, Schultz CW, Thomas A, Zenke FT, Pommier Y, Novel and highly potent ATR inhibitor M4344 kills cancer cells with replication stress, and enhances the chemotherapeutic activity of widely used DNA damaging agents. Mol. Cancer Ther 20, 1431–1441 (2021). [PubMed: 34045232]
33. Gyorffy B, Lánczky A, Szállási Z, Implementing an online tool for genome-wide validation of survival-associated biomarkers in ovarian-cancer using microarray data from 1287 patients. Endocr. Relat. Cancer 19, 197–208 (2012). [PubMed: 22277193]
34. Maity J, Horibata S, Zurcher G, Lee JM, Targeting of RecQ helicases as a novel therapeutic strategy for ovarian cancer. Cancers (Basel) 14, 1219 (2022). [PubMed: 35267530]
35. Birkbak NJ, Li Y, Pathania S, Greene-Colozzi A, Dreze M, Bowman-Colin C, Sztupinszki Z, Krzystanek M, Diossy M, Tung N, Ryan PD, Garber JE, Silver DP, Iglehart JD, Wang ZC, Szuts D, Szallasi Z, Richardson AL, Overexpression of BLM promotes DNA damage and increased sensitivity to platinum salts in triple-negative breast and serous ovarian cancers. Ann. Oncol 29, 903–909 (2018). [PubMed: 29452344]
36. Walton MI, Eve PD, Hayes A, Henley AT, Valenti MR, De Haven Brandon AK, Box G, Boxall KJ, Tall M, Swales K, Matthews TP, McHardy T, Lainchbury M, Osborne J, Hunter JE, Perkins ND, Aherne GW, Reader JC, Raynaud FI, Eccles SA, Collins I, Garrett MD, The clinical development candidate CCT245737 is an orally active CHK1 inhibitor with preclinical activity in RAS mutant NSCLC and Eμ-MYC driven B-cell lymphoma. Oncotarget 7, 2329–2342 (2016). [PubMed: 26295308]
37. Ahmed AA, Etemadmoghadam D, Temple J, Lynch AG, Riad M, Sharma R, Stewart C, Fereday S, Caldas C, DeFazio A, Driver mutations in TP53 are ubiquitous in high grade serous carcinoma of the ovary. J. Pathol 221, 49–56 (2010). [PubMed: 20229506]
38. Zhu L, Liu J, Chen J, Zhou Q, The developing landscape of combinatorial therapies of immune checkpoint blockade with DNA damage repair inhibitors for the treatment of breast and ovarian cancers. J. Hematol. Oncol 14, 206 (2021). [PubMed: 34930377]
39. Lheureux S, Oaknin A, Garg S, Bruce JP, Madariaga A, Dhani NC, Bowering V, White J, Accardi S, Tan Q, Braunstein M, Karakasis K, Cirlan I, Pedersen S, Li T, Farinas-Madrid L, Lee YC, Liu ZA, Pugh TJ, Oza AM, EVOLVE: A multicenter open-label single-arm clinical and translational phase II trial of cediranib plus olaparib for ovarian cancer after PARP inhibition progression. Clin. Cancer Res 26, 4206–4215 (2020). [PubMed: 32444417]
40. Xu H, George E, Kinose Y, Kim H, Shah JB, Peake JD, Ferman B, Medvedev S, Murtha T, Barger CJ, Devins KM, D'Andrea K, Wubbenhorst B, Schwartz LE, Hwang W-T, Mills GB, Nathanson KL, Karpf AR, Drapkin R, Brown EJ, Simpkins F, CCNE1 copy number is a biomarker for response to combination WEE1-ATR inhibition in ovarian and endometrial cancer models. Cell Rep. Med 2, 100394 (2021).
41. Ditano JP, Donahue KL, Tafe LJ, McCleery CF, Eastman A, Sensitivity of cells to ATR and CHK1 inhibitors requires hyperactivation of CDK2 rather than endogenous replication stress or ATM dysfunction. Sci. Rep 11, 7077 (2021). [PubMed: 33782497]
42. Sakurikar N, Thompson R, Montano R, Eastman A, A subset of cancer cell lines is acutely sensitive to the Chk1 inhibitor MK-8776 as monotherapy due to CDK2 activation in S phase. Oncotarget 7, 1380–1394 (2016). [PubMed: 26595527]
43. Konecny GE, Wang C, Hamidi H, Winterhoff B, Kalli KR, Dering J, Ginther C, Chen H-W, Dowdy S, Cliby W, Gostout B, Podratz KC, Keeney G, Wang H-J, Hartmann LC, Slamon DJ, Goode EL, Prognostic and therapeutic relevance of molecular subtypes in high-grade serous ovarian cancer. J. Natl. Cancer Inst 106, dju249 (2014).
44. Lampert EJ, Cimino-Mathews A, Lee JS, Nair J, Lee M-J, Yuno A, An D, Trepel JB, Ruppin E, Lee J-M, Clinical outcomes of prexasertib monotherapy in recurrent *BRCA* wild-type high-grade serous ovarian cancer involve innate and adaptive immune responses. J. Immunother. Cancer 8, e000516 (2020).
45. Verhaak RG, Tamayo P, Yang JY, Hubbard D, Zhang H, Creighton CJ, Fereday S, Lawrence M, Carter SL, Mermel CH, Kostic AD, Etemadmoghadam D, Saksena G, Cibulskis K, Duraisamy S, Levanon K, Sougnez C, Tsherniak A, Gomez S, Onofrio R, Gabriel S, . Chin N. Zhang PT Zhang Spellman, Y., Akbani R, Hoadley KA, Kahn A, Kobel M, Huntsman D, Soslow RA, Defazio A,

Birrer MJ, Gray JW, Weinstein JN, Bowtell DD, Drapkin R, Mesirov JP, Getz G, Levine DA, Meyerson M; Cancer Genome Atlas Research Network, Prognostically relevant gene signatures of high-grade serous ovarian carcinoma. J. Clin. Invest 123, 517–525 (2013). [PubMed: 23257362]

46. Etemadmoghadam D, Defazio A, Beroukhim R, Mermel C, George J, Getz G, Tothill R, Okamoto A, Raeder MB, Harnett P, Integrated genome-wide DNA copy number and expression analysis identifies distinct mechanisms of primary chemoresistance in ovarian carcinomas. Clin. Cancer Res 15, 1417–1427 (2009). [PubMed: 19193619]
47. Sapoznik S, Aviel-Ronen S, Bahar-Shany K, Zadok O, Levanon K, CCNE1 expression in high grade serous carcinoma does not correlate with chemoresistance. Oncotarget 8, 62240–62247 (2017). [PubMed: 28977941]
48. Do KT, Kochupurakkal B, Kelland S, de Jonge A, Hedglin J, Powers A, Quinn N, Gannon C, Vuong L, Parmar K, Lazaro JB, D'Andrea AD, Shapiro GI, Phase 1 combination study of the CHK1 inhibitor prexasertib and the PARP inhibitor olaparib in high-grade serous ovarian cancer and other solid tumors. Clin. Cancer Res 27, 4710–4716 (2021). [PubMed: 34131002]
49. Sengupta S, Robles AI, Linke SP, Sinogeeva NI, Zhang R, Pedeux R, Ward IM, Celeste A, Nussenzweig A, Chen J, Halazonetis TD, Harris CC, Functional interaction between BLM helicase and 53BP1 in a Chk1-mediated pathway during S-phase arrest. J. Cell Biol 166, 801–813 (2004). [PubMed: 15364958]
50. Karst AM, Jones PM, Vena N, Ligon AH, Liu JF, Hirsch MS, Etemadmoghadam D, Bowtell DD, Drapkin R, Cyclin E1 deregulation occurs early in secretory cell transformation to promote formation of fallopian tube-derived high-grade serous ovarian cancers. Cancer Res. 74, 1141–1152 (2014). [PubMed: 24366882]
51. Marshall AE, Roes MV, Passos DT, DeWeerd MC, Chaikovsky AC, Sage J, Howlett CJ, Dick FA, *RB1* deletion in retinoblastoma protein pathway-disrupted cells results in DNA damage and cancer progression. Mol. Cell. Biol 39, e00105-19 (2019).
52. Toledo L, Neelsen KJ, Lukas J, Replication catastrophe: When a checkpoint fails because of exhaustion. Mol. Cell 66, 735–749 (2017). [PubMed: 28622519]
53. D'Andrea AD, Mechanisms of PARP inhibitor sensitivity and resistance. DNA Repair (Amst) 71, 172–176 (2018). [PubMed: 30177437]
54. Dreyer SB, Upstill-Goddard R, Paulus-Hock V, Paris C, Lampraki EM, Dray E, Serrels B, Caligiuri G, Rebus S, Plenker D, Galluzzo Z, Brunton H, Cunningham R, Tesson M, Nourse C, Bailey UM, Jones M, Moran-Jones K, Wright DW, Duthie F, Oien K, Evers L, McKay CJ, McGregor GA, Gulati A, Brough R, Bajrami I, Pettitt S, Dziubinski ML, Candido J, Balkwill F, Barry ST, Grutzmann R, Rahib L; Glasgow Precision Oncology Laboratory; Australian Pancreatic Cancer Genome Initiative, Johns A, Pajic M, Froeling FEM, Beer P, Musgrove EA, Petersen GM, Ashworth A, Frame MC, Crawford HC, Simeone DM, Lord C, Mukhopadhyay D, Pilarsky C, Tuveson DA, Cooke SL, Jamieson NB, Morton JP, Sansom OJ, Bailey PJ, Biankin AV, Chang DK, Targeting DNA damage response and replication stress in pancreatic cancer. Gastroenterology 160, 362–377.e13 (2021). [PubMed: 33039466]
55. Leffers N, Gooden MJ, de Jong RA, Hoogeboom B-N, ten Hoor KA, Hollema H, Boezen HM, van der Zee AG, Daemen T, Nijman HW, Prognostic significance of tumor-infiltrating T-lymphocytes in primary and metastatic lesions of advanced stage ovarian cancer. Cancer Immunol. Immunother 58, 449–459 (2009). [PubMed: 18791714]
56. Sato E, Olson SH, Ahn J, Bundy B, Nishikawa H, Qian F, Jungbluth AA, Frosina D, Gnjatic S, Ambrosone C, Intraepithelial $CD8^+$ tumor-infiltrating lymphocytes and a high $CD8^+$/regulatory T cell ratio are associated with favorable prognosis in ovarian cancer. Proc. Natl. Acad. Sci. U.S.A 102, 18538–18543 (2005). [PubMed: 16344461]
57. Au-Yeung G, Bressel M, Prall O, Surace D, Andrews J, Mongta S, Lee YC, Gao B, Meniawy T, Baron-Hay SE, Black AJ, Kichenadasse G, Ananda S, Fox P, Bowtell D, Mileshkin LR, IGNITE: A phase II signal-seeking trial of adavosertib targeting recurrent high-grade, serous ovarian cancer with cyclin E1 overexpression with and without gene amplification. J. Clin. Oncol 40, 5515–5515 (2022).
58. Huang TT, Brill E, Nair JR, Zhang X, Wilson KM, Chen L, Thomas CJ, Lee J-M, Targeting the PI3K/mTOR pathway augments CHK1 inhibitor–Induced replication stress and antitumor activity in high-grade serous ovarian cancer. Cancer Res. 80, 5380–5392 (2020). [PubMed: 32998994]

59. Yamamoto N, Nokihara H, Yamada Y, Goto Y, Tanioka M, Shibata T, Yamada K, Asahina H, Kawata T, Shi X, Tamura T, A phase I, dose-finding and pharmacokinetic study of olaparib (AZD2281) in Japanese patients with advanced solid tumors. Cancer Sci. 103, 504–509 (2012). [PubMed: 22145984]
60. Chou TC, Theoretical basis, experimental design, and computerized simulation of synergism and antagonism in drug combination studies. Pharmacol. Rev 58, 621–681 (2006). [PubMed: 16968952]
61. Huang TT, Lampert EJ, Coots C, Lee JM, Targeting the PI3K pathway and DNA damage response as a therapeutic strategy in ovarian cancer. Cancer Treat. Rev 86, 102021 (2020). [PubMed: 32311593]
62. Hu P, Beresten SF, van Brabant AJ, Ye TZ, Pandolfi PP, Johnson FB, Guarente L, Ellis NA, Evidence for BLM and Topoisomerase IIIα interaction in genomic stability. Hum. Mol. Genet 10, 1287–1298 (2001). [PubMed: 11406610]
63. Rustin GJ, Vergote I, Eisenhauer E, Pujade-Lauraine E, Quinn M, Thigpen T, du Bois A, Kristensen G, Jakobsen A, Sagae S, Greven K, Parmar M, Friedlander M, Cervantes A, Vermorken J, Gynecological Cancer I, Definitions for response and progression in ovarian cancer clinical trials incorporating RECIST 1.1 and CA 125 agreed by the Gynecological Cancer Intergroup (GCIG). Int. J. Gynecol. Cancer 21, 419–423 (2011). [PubMed: 21270624]
64. Rose PG, Tian C, Bookman MA, Assessment of tumor response as a surrogate endpoint of survival in recurrent/platinum-resistant ovarian carcinoma: A gynecologic Oncology Group study. Gynecol. Oncol 117, 324–329 (2010). [PubMed: 20185168]
65. Ritchie ME, Phipson B, Wu D, Hu Y, Law CW, Shi W, Smyth GK, limma powers differential expression analyses for RNA-sequencing and microarray studies. Nucleic Acids Res. 43, e47 (2015). [PubMed: 25605792]
66. Corchete LA, Rojas EA, Alonso-Lopez D, De Las Rivas J, Gutierrez NC, Burguillo FJ, Systematic comparison and assessment of RNA-seq procedures for gene expression quantitative analysis. Sci. Rep 10, 19737 (2020). [PubMed: 33184454]
67. Butler A, Hoffman P, Smibert P, Papalexi E, Satija R, Integrating single-cell transcriptomic data across different conditions, technologies, and species. Nat. Biotechnol 36, 411–420 (2018). [PubMed: 29608179]
68. Tothill RW, Tinker AV, George J, Brown R, Fox SB, Lade S, Johnson DS, Trivett MK, Etemadmoghadam D, Locandro B, Traficante N, Fereday S, Hung JA, Chiew YE, Haviv I, Gertig D, DeFazio A, Bowtell DD, Novel molecular subtypes of serous and endometrioid ovarian cancer linked to clinical outcome. Clin. Cancer Res 14, 5198–5208 (2008). [PubMed: 18698038]
69. Győrffy B, Survival analysis across the entire transcriptome identifies biomarkers with the highest prognostic power in breast cancer. Comput. Struct. Biotechnol. J 19, 4101–4109 (2021). [PubMed: 34527184]

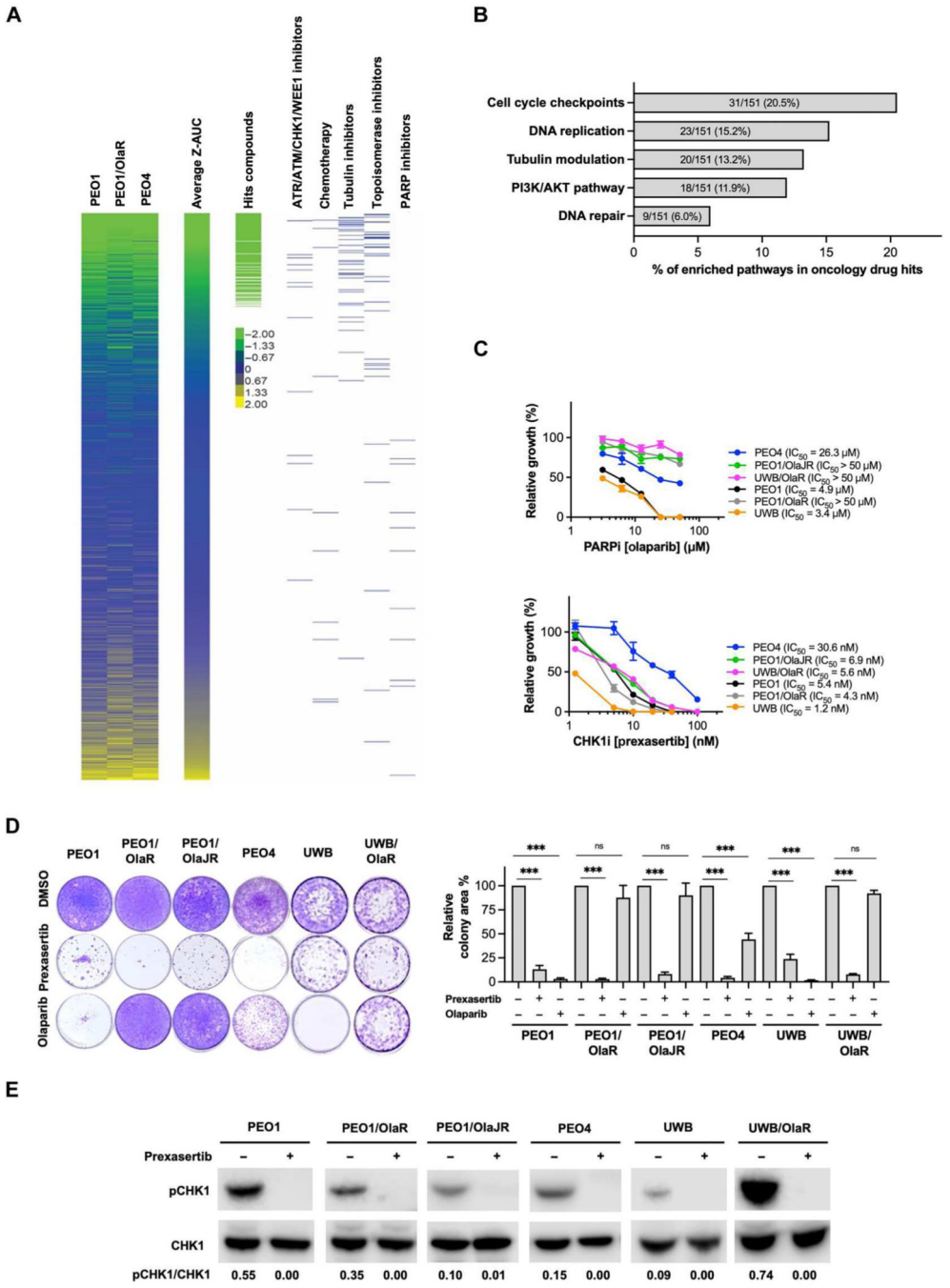

Fig. 1. In vitro drug screens identify ATR/CHK1 inhibitors as active drugs in both PARPi-sensitive and -resistant *BRCA*-mutant HGSC cell lines.

(**A**) Heatmap of ranked drug activities for PARPi-sensitive and -resistant *BRCA2*-mutant HGSC cell lines, including PARPi-sensitive PEO1, PARPi-resistant PEO1/OlaR, and de novo PARPi–resistant PEO4 cells. Single-agent drug activities were screened using the MIPE 5.0 library of approved and investigational drugs (oncology drugs, $n = 1082$). Activity scores are based on Z-AUC. The average Z-AUC value >0 indicates inactive drugs, whereas <0 represents active drugs (15). The most active drugs based on their primary mechanisms

of action, chemotherapy drugs for ovarian cancer, and PARPis are shown on the right. (**B**) Mechanistic classes enriched among highly active drugs are shown by the Reactome database (https://reactome.org/) analysis. (**C** and **D**) Cell growth was validated using XTT (C) and colony-forming assays (D) in *BRCA1*-null UWB, *BRCA2*-mutant PEO1, *BRCA2* reversion mutation PEO4, and acquired PARPi–resistant UWB (UWB/OlaR) and PEO1 (PEO1/OlaR and PEO1/OlaJR) cell lines. (C) Short-term cell growth was evaluated by the XTT assay. Cells were treated with the PARPi olaparib (top) or the CHK1i prexasertib (bottom) at the indicated doses for 72 hours. IC_{50} values were calculated using GraphPad Prism v7.1. (D) Long-term cell proliferation was examined using colony-forming assays. Cells were seeded at low density and treated with prexasertib (0.5 nM for UWB and 5 nM for all other cell lines) or olaparib (10 μM) and grown for 12 to 15 days. Colonies were visualized by 0.01% (w/v) crystal violet staining. Quantification was performed by ImageJ. (**E**) On-target effect of prexasertib was assessed by immunoblotting of p-CHK1 (S296) and total CHK1. Densitometric values of p-CHK1 (S296) relative to total CHK1 are shown. All experiments were repeated at least in triplicate, and data are shown as means ± SEM. ***$P < 0.001$; ns, not significant. CHK1i, CHK1 inhibitor; HGSC, high-grade serous ovarian cancer; PARPi, PARP inhibitor; UWB, UWB1.289; *Z*-AUC, *Z*-transformed area under the curve.

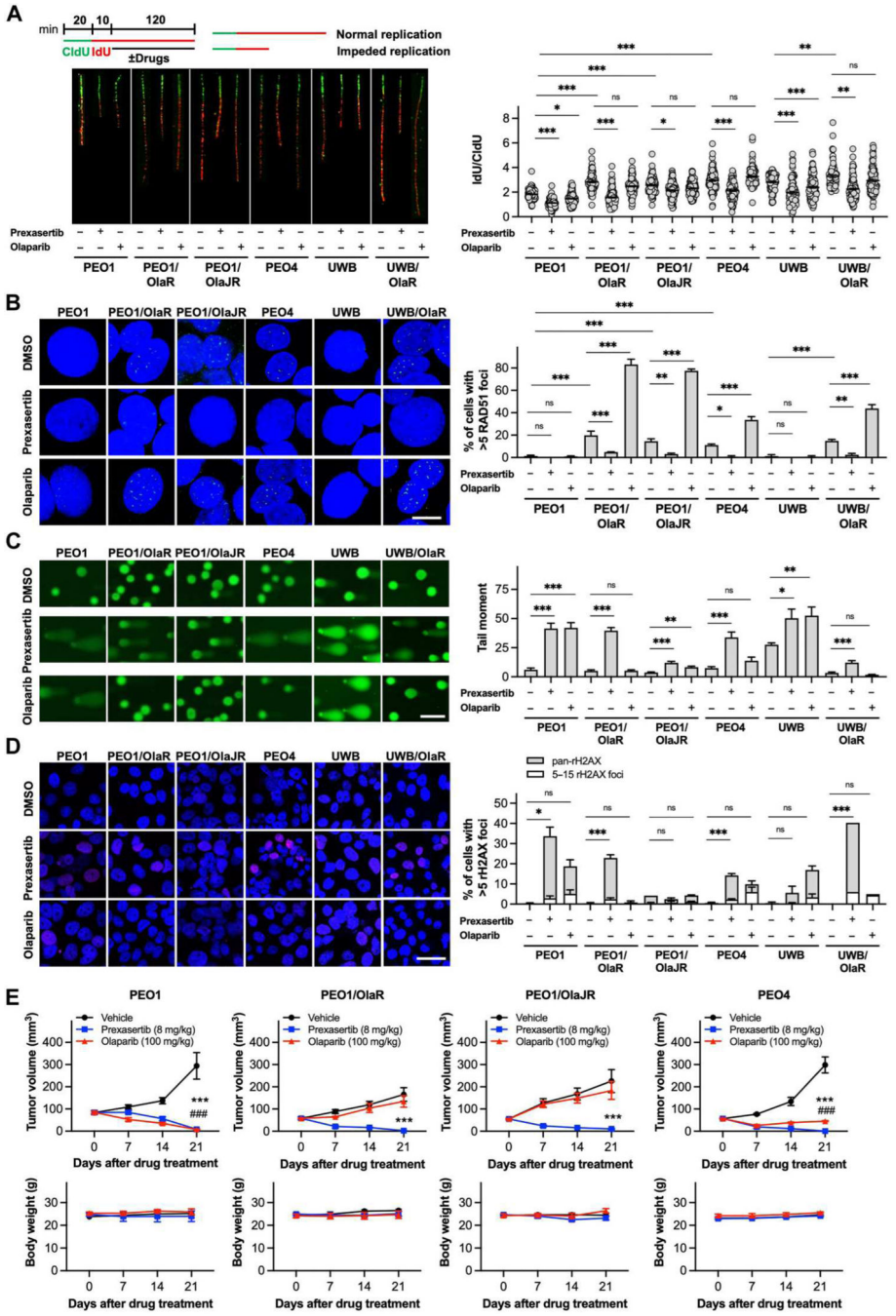

Fig. 2. CHK1i monotherapy disrupts fork stabilization and HR restoration in PARPi-resistant *BRCA*-deficient HGSC in vitro and in vivo models.

(**A**) Replication fork stability in PARPi-sensitive (PEO1 and UWB), acquired PARPi–resistant (PEO1/OlaR, PEO1/OlaJR, and UWB/OlaR), and de novo PARPi–resistant (PEO4) cells was measured by DNA fiber assays. Cells were incubated with CldU and then IdU and coincubated with prexasertib (20 nM) or olaparib (20 μM). Representative images are shown (left). Dot plots of IdU (red) to CldU (green) tract length ratios in treated cells are plotted (right). A lower ratio of IdU/CldU indicates fork destabilization and

hindered replication, suggesting higher replication stress. (**B** to **D**) Cells were treated with prexasertib (5 nM for all cell lines except 0.5 nM for UWB) or olaparib (10 μM) for 48 hours. (B) HR status was measured by immunofluorescence staining of RAD51 foci (green). Representative images are shown (left), and the percentage of cells with >5 RAD51 foci is plotted (right). Scale bar, 40 μm. DNA damage was examined by (C) the alkaline comet assay and (D) immunofluorescence staining of γH2AX foci (a marker of DNA double-strand breaks). (C) Representative images of DNA fragments are shown (left), and the percentage of DNA in comet tails is plotted (right). Scale bar, 100 μm. (D) The γH2AX foci (pink) were assessed by immunofluorescence staining. Cell nuclei were stained with 4′,6-diamidino-2-phenylindole (blue). Representative images are shown (left). The percentage of cells with 5 to 15 γH2AX foci, representing cells with DNA damage, and cells with pan-γH2AX staining, indicating cell apoptosis, is plotted (right). Scale bar, 50 μm. The above experiments were repeated, at least in triplicate, and data are shown as means ± SEM. *$P < 0.05$; **$P < 0.01$; ***$P < 0.001$. (**E**) In vivo assessment of prexasertib (8 mg/kg) and olaparib (100 mg/kg) in PARPi-sensitive and PARPi-resistant *BRCA2*-mutant HGSC xenograft tumors ($n = 5$ per group). Tumor volumes are plotted (top). The body weight of mice was measured once per week to monitor drug tolerance (bottom). Data are shown as means ± SEM. ***$P < 0.001$, prexasertib versus vehicle; ###$P < 0.001$, olaparib versus vehicle. CldU, 5-chloro-2′-deoxyuridine; HR, homologous recombination; IdU, 5-iodo-2′-deoxyuridine.

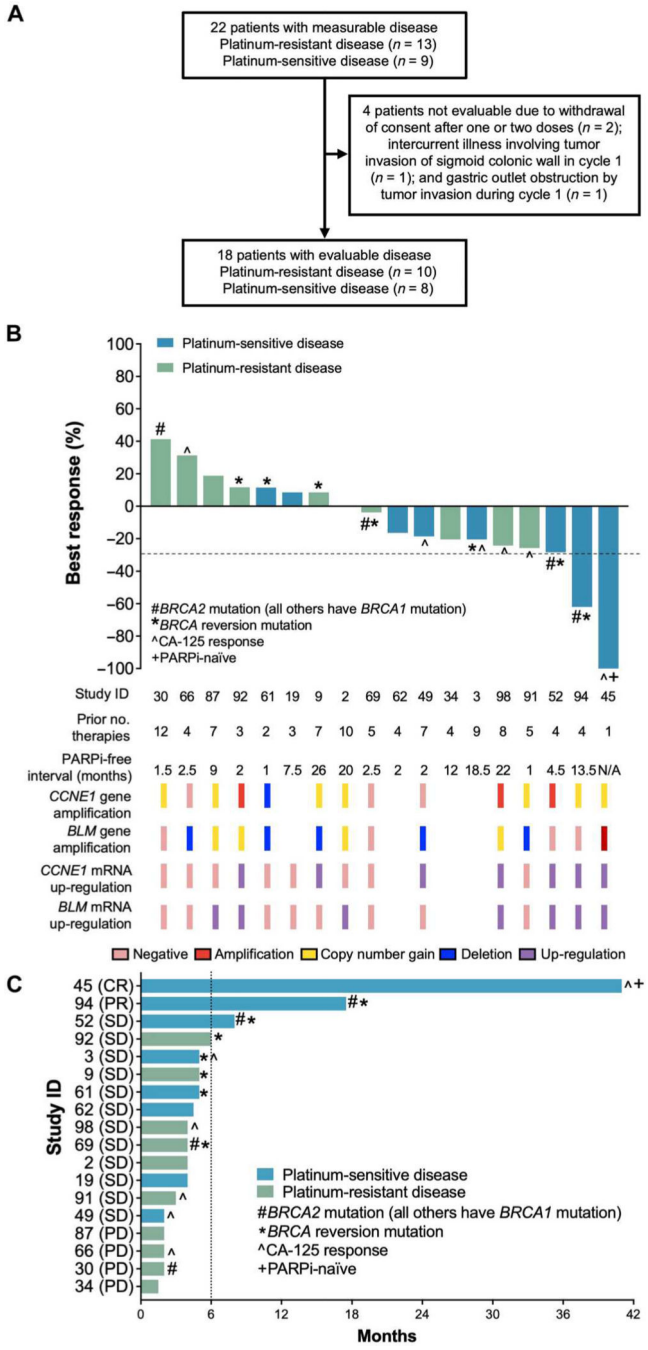

Fig. 3. Clinical trial design and activity of prexasertib in *BRCA*-mutant HGSC.

(**A**) The CONSORT flow diagram. In total, there were 22 patients enrolled in the study, with 18 evaluable for RECIST response. (**B**) Waterfall plot showing the best response to treatment in 18 evaluable patients. Best RECIST responses (percentage change from baseline in tumor size) are shown according to the number of previous treatments, PARPi-free interval, presence of *BLM* and *CCNE1* gene amplification/gain/deletion, and the presence of *BLM* and *CCNE1* mRNA up-regulation in pretreatment biopsy samples. The horizontal dotted line indicates the threshold for PR (30% reduction in tumor size from

baseline). (**C**) Swimmer plot showing duration of treatment for 18 evaluable patients. The vertical dotted line indicates the threshold for clinical benefit (CR + PR + SD ≥ 6 months). The cross symbol (+) in (B) and (C) indicates the PARPi-naïve, CR patient. The hash symbol (#) represents cancers with *BRCA2* mutation; all others have *BRCA1* mutations. Asterisks (*) indicate cancers with *BRCA* reversion mutations detected (see table S4 for more details). The caret symbol (^) indicates patients with CA-125 response (see fig. S3C for more details). RECIST, Response Evaluation Criteria in Solid Tumors; CR, complete response; PR, partial response; SD, stable disease; PD, progression of disease; N/A, not applicable; no., number.

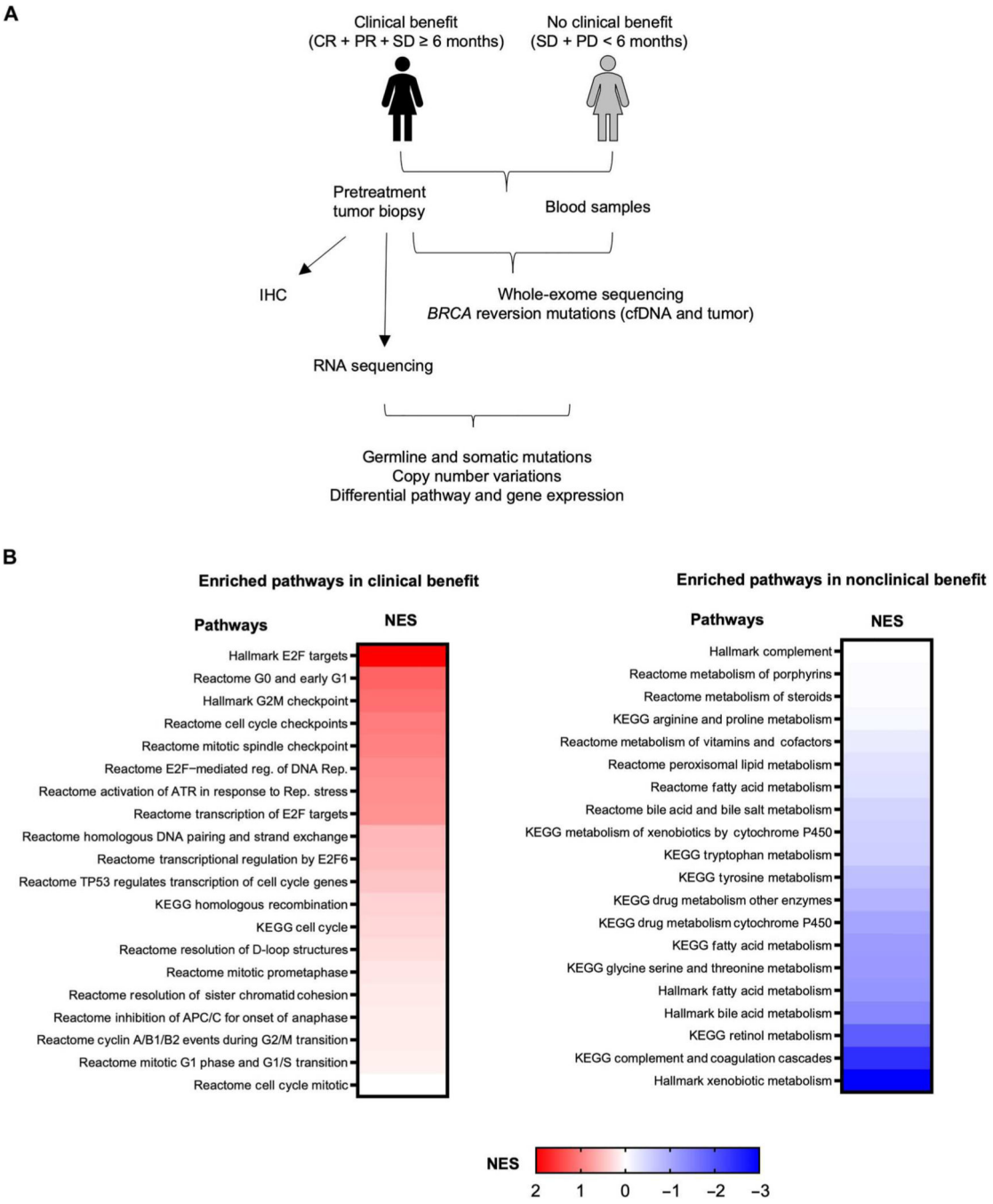

Fig. 4. Exploratory biomarker analyses reveal differentially up-regulated pathways associated with clinical benefit.

(**A**) Schema for exploratory biomarker analyses. (**B**) Gene set enrichment analysis by Hallmark, KEGG, and Reactome databases of RNA-seq data shows up-regulated (red) and down-regulated (blue) gene set pathways in those with clinical benefit (left) but not in those with no clinical benefit (right). cfDNA, cell-free DNA; IHC, immunohistochemistry; KEGG, Kyoto Encyclopedia of Genes and Genomes; NES, normalized enrichment score; Rep., replication.

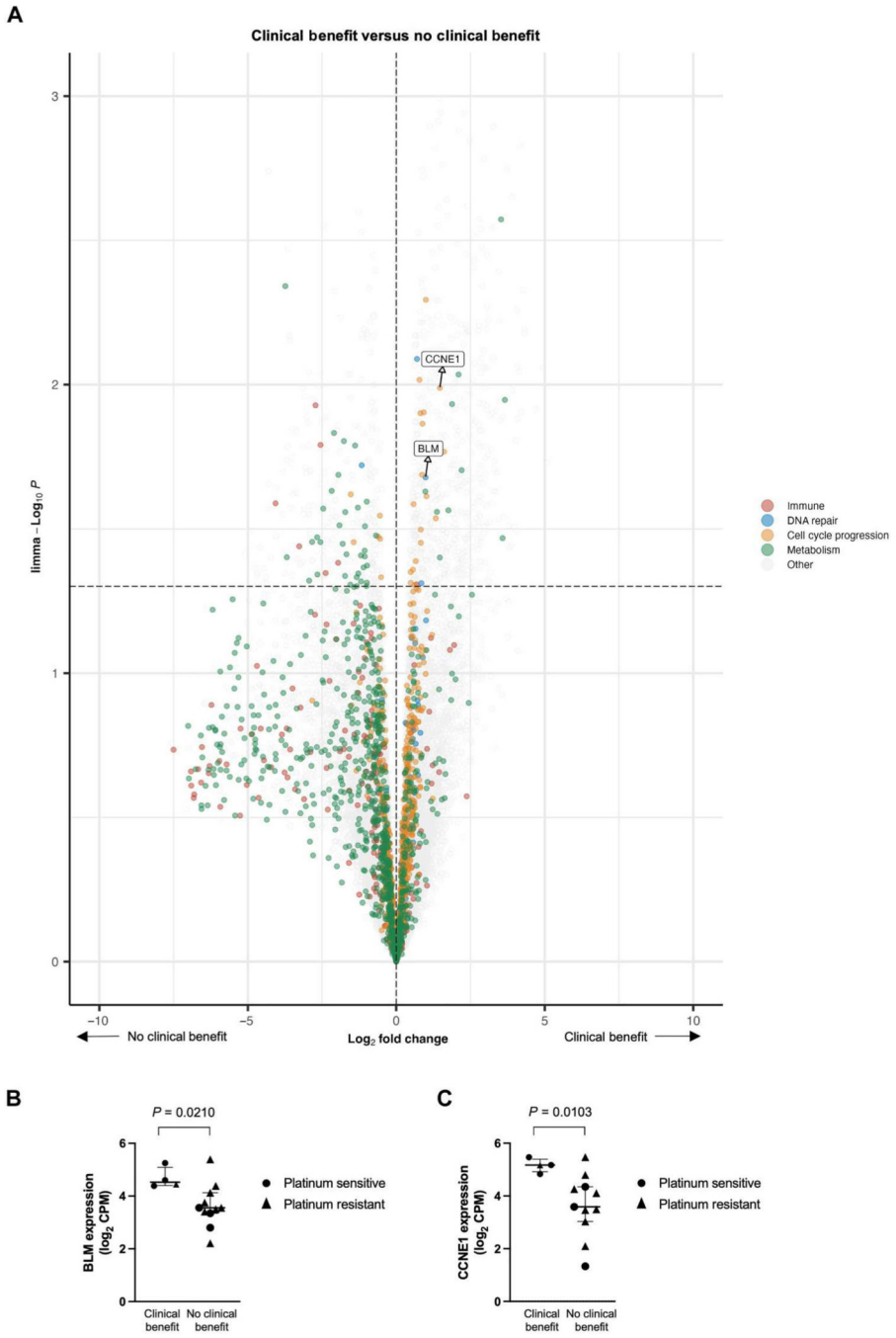

Fig. 5. High mRNA expression of *BLM* and *CCNE1* is associated with clinical benefit.

(**A**) The mRNA expression of genes was analyzed from RNA-seq data from patients with clinical benefit ($n = 4$) versus those with no clinical benefit ($n = 11$). The x axis shows $\log_2$ fold change (>0 indicates genes enriched in patients with clinical benefit, whereas <0 indicates genes enriched in patients with no clinical benefit). The y axis shows the Wilcoxon $-\log_{10} P$ values, and the horizontal dotted line represents a significance threshold of $P = 0.05$, with significantly enriched genes falling above the line. (**B** and **C**) The mRNA expression of RecQ helicase BLM (B) and CCNE1 (C) is shown in patients with clinical

benefit and those with no clinical benefit. Lines represent median with 95% confidence interval. CPM, counts per million.

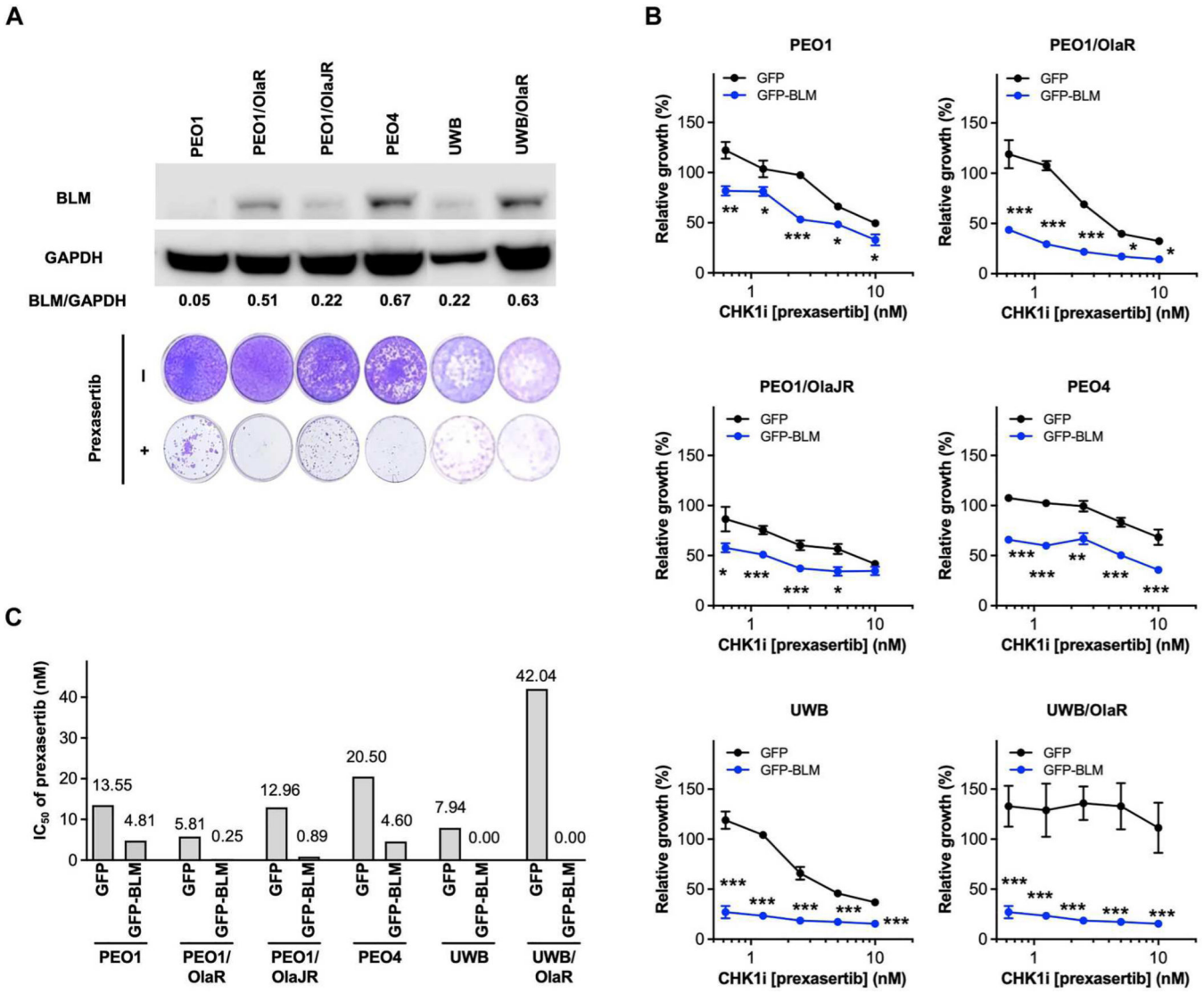

Fig. 6. BLM overexpression increases the sensitivity of CHK1i in HGSC cell lines.

(**A**) Basal abundances of BLM in parental (*BRCA*-mutant PEO1 and UWB), acquired PARPi–resistant (PEO1/OlaR, PEO1/OlaJR, and UWB/OlaR), and de novo PARPi–resistant (PEO4) cell lines were analyzed by immunoblotting. Densitometric values of BLM relative to glyceraldehyde-3-phosphate dehydrogenase (GAPDH) (top) and representative colony formation images of cells with or without prexasertib treatment are shown (bottom). (**B** and **C**) Cells transfected with *BLM* overexpression plasmids for 48 hours were treated with or without prexasertib for another 48 hours. Cell viability was measured by the XTT assay (B). IC_{50} values (C) from (B) were calculated using GraphPad Prism v7.1. Experiments were repeated, at least in triplicate, and data are shown as means ± SEM. *$P < 0.05$; **$P < 0.01$; ***$P < 0.001$.

Table 1.

Baseline patient characteristics (*n* = 22).

Platinum-sensitive disease: disease recurrence ≥6 months after completing platinum-based therapy. Platinum-resistant disease: disease recurrence <6 months after completing platinum-based therapy. Primary platinum-resistant: disease progression <6 months after completing the first-line platinum-based therapy. Secondary platinum-resistant: disease progression ≥6 months after the first platinum-based therapy but <6 months after the last platinum-based therapy for platinum-sensitive relapse. No patients were refractory to their first platinum or PARPi treatment. BRCA, breast cancer gene; CA-125, cancer antigen 125; CLIA, Clinical Laboratory Improvement Amendments; CTLA-4, cytotoxic T lymphocyte–associated protein 4; ECOG, Eastern Cooperative Oncology Group; HRD, homologous recombination deficiency; *N*, number; PARPi, poly(ADP-ribose) polymerase inhibitor; PD-L1, programmed death-ligand 1; TKI, tyrosine kinase inhibitor; VEGFR, vascular endothelial growth factor receptor.

Characteristics	Number of patients (% total)
Age in years, median (range)	56.4 (35.7–74.8)
BRCA mutation *	
BRCA1	14 germline, 1 somatic
BRCA2	6 germline, 1 somatic
ECOG performance status, *N*(%)	
0	6 (27%)
1	15 (68%)
2	1 (5%)
Platinum status, *N*(%)	
Platinum-sensitive disease	9 (41%)
Platinum-resistant disease	13 (59%)
Primary platinum-resistant	0
Secondary platinum-resistant	13 (59%)
Median number of prior systemic therapy regimens (range)	5 (1–12)
Median among platinum-sensitive	4 (1–5)
Median among platinum-resistant	8 (3–12)
Prior cytotoxic chemotherapy, *N*(%)	22 (100%)
Prior radiotherapy, *N*(%)	2 (9%)
Prior PARP inhibitor(s), *N*(%)	21 (95%)
Treatment setting only	6 (29%)
Maintenance setting only (upfront/platinum-sensitive recurrent setting)	13 (62%)
Both treatment and maintenance settings	2 (9%)
Median PARPi duration in months (range)	9 (3.5–48)
Median PARPi-free interval before starting prexasertib (range)	4.5 (1–26)
Prior angiogenic(s), *N*(%)	17 (77%)
Bevacizumab only	13 (59%)
VEGFR TKI (cediranib) only	3 (14%)

Characteristics	Number of patients (% total)
Both bevacizumab (maintenance) and cediranib (treatment)	1 (5%)
Prior immune checkpoint inhibitor(s), *N* (%)	9 (41%)
Anti–PD-L1 inhibitor only	8 (36%)
Anti–PD-L1 inhibitor + anti–CTLA-4 inhibitor (ipilimumab)	1 (5%)
Baseline CA-125 concentration	
Normal (1.9–16.3 U/ml), *N* (%)	1 (5%)
Abnormal (>16.3 U/ml), *N* (%)	21 (95%)

* Information on the status of *BRCA* mutations was obtained from CLIA-certified comprehensive commercial *BRCA* or HRD testing done before enrollment.

Table 2.

Treatment-related adverse events.

Patients could be counted under more than one preferred term.

Adverse event	Maximum grade in all patients (*n* = 22)		
	1–2	3	4
Hematologic	Number of patients (% total)		
Anemia	21 (95%)	1 (5%)	0
Neutropenia *	1 (5%)	3 (14%)	15 (68%)
Leukopenia	5 (23%)	9 (41%)	5 (23%)
Thrombocytopenia	14 (64%)	1 (5%)	2 (9%)
Lymphopenia	11 (50%)	6 (27%)	0
Febrile neutropenia	0	1 (5%)	0
Nonhematologic	Number of patients (% total)		
Fatigue	11 (50%)	0	0
Fever	4 (18%)	0	0
Allergic reaction	2 (9%)	0	0
Headache	1 (5%)	0	0
Nausea	11 (50%)	1 (5%)	0
Vomiting	5 (23%)	1 (5%)	0
Rash (acneiform, maculopapular)	4 (18%)	0	0
Diarrhea	4 (18%)	0	0
Constipation	3 (14%)	0	0
Abdominal pain	2 (9%)	0	0
Anorexia	2 (9%)	0	0
Oral mucositis	1 (5%)	0	0

* Sixteen of 18 (89%) patients with grade 3/4 neutropenia on cycle 1 day 8 received prophylactic growth factors for subsequent treatments to avoid treatment delay or dose reductions.